Yusuf Olanrewaju Busari[1,2], Yupiter Harangan Prasada Manurung[1]

WELDED HIGH STRENGTH LOW ALLOY STEEL INFLUENCE ON FATIGUE CRACK PROPAGATION USING LEFM: A PRACTICAL AND THEMATIC REVIEW

UTICAJ ZAVARENOG NISKOLEGIRANOG ČELIKA POVIŠENE ČVRSTOĆE NA RAST ZAMORNE PRSLINE PRIMENOM LEML: PRAKTIČAN I TEMATSKI PREGLED

Pregledni rad / Review paper
UDK /UDC:

Rad primljen / Paper received: 6.05.2020

Adresa autora / Author's address:
[1)] Smart Manufacturing Research Institute (SMRI), Faculty of Mechanical Engineering, Universiti Teknologi MARA (UiTM), Shah Alam, Malaysia
[2)] Materials & Metallurgical Engineering Department, University of Ilorin, Ilorin, Nigeria
email: yupiter.manurung@uitm.edu.my

Keywords
- fatigue crack growth
- high strength low-alloyed steel (HSLA)
- linear elastic fracture mechanics (LEFM)
- finite element method (FEM)
- residual stress

Abstract

The application of linear elastic fracture mechanics approach in analysing fatigue crack growth rates in welded high strength steels is reviewed. A systematic literature review is undertaken in order to demonstrate the efficacy of small test specimens in testing welded structures for fatigue crack life. Experiments demonstrate that use of conventional specimen testing for probabilistic fatigue crack growth rate in welded steel might overlook the effect of induced residual stress. Firstly, an ideal fatigue crack propagation life prediction technique for welded high strength steels that includes fatigue crack driving force with established methods is analysed, since real geometries are difficult to properly represent in analytical and numerical applications. In the second part are investigated essential experimental cases of welds in high strength steel and the load spectrum and geometry for fatigue crack growth rate based on LEFM. The third part covers the current state of LEFM model for fatigue crack growth rate (FCGR) using FEM. This approach considers the induced residual welding effect for the purpose of reliable integrity assessment. This review also focuses on the impact of test specimen inconsistency on fatigue crack growth rate evaluation. Implementing the standardized test specimen may complement the creation of new techniques to avoid weld stress relaxation of the critical welded high strength steel structure for probabilistic fatigue crack growth rate evaluation.

Ključne reči
- rast zamorne prsline
- niskolegirani čelik povišene čvrstoće (HSLA)
- linearno elastična mehanika loma (LEFM)
- metoda konačnih elemenata (FEM)
- zaostali napon

Izvod

U radu je analizirana primena principa linearno-elastične mehanike loma na ocenu brzine rasta zamorne prsline u zavarenim konstrukcijama od niskolegiranih čelika povišene čvrstoće. Dat je sistematski pregled literature sa ciljem da demonstrira efikasnost malih epruveta za ispitivanja zamornog veka zavarenih konstrukcija. Eksperimentalna ispitivanja su pokazala da se kod primene uobičajenih epruveta za probabilističku ocenu zamornog veka zavarenih konstrukcija često može prevideti uticaj zaostalih napona. Idealna metoda za procenu preostalog veka konstrukcija sa zamornom prslinom za čelike povišene čvrstoće, ovde analizirana, bi pre svega trebalo da uzme u obzir silu rasta prsline, s obzirom da realnu geometriju nije uvek jednostavno uvesti u analitički ili numerički proračun. U drugom delu rada se posmatraju uopšteni slučajevi ispitivanja ovakvih čelika, kod kojih su spektar opterećenja, geometrija i brzina rasta zamorne prsline zasnovani na LEML. U trećem delu je obrađeno trenutno stanje modela za simulaciju rasta zamorne prsline (FCGR) primenom FEM. Ovaj pristup uzima u obzir i uticaj zaostalih napona na integritet konstrukcije. U preglednom radu se posmatra i uticaj nekonzistentnosti epruvete na ocenu brzine rasta zamorne prsline. Primena standardnih epruveta može doprineti razvoju novih tehnika za probabilističku ocenu brzine rasta zamorne prsline, kojima se smanjuje prisustvo zaostalih napona u kritičnim mestima zavarenih konstrukcija od čelika povišene čvrstoće.

INTRODUCTION

Most welded steel structures are expected to meet robust quality assurance caused by huge investment and safety requirements. Nevertheless, cracks and notches in welds are likely to be present and to be sources of stress raisers /1/, prone to fatigue crack growth /2/. Despite vast research, fatigue of welded structural steels is still a very complex phenomenon. One of many approaches is linear elastic fracture mechanics providing safe-life design method taking into account pre-existing flaws by considering the stress field around crack tip, /3/. The parameter used thereby is the stress intensity factor (SIF).

There are many approaches for determining fatigue life but to generate fatigue properties for damage tolerant design and fatigue crack growth rate (FCGR), testing is performed at a given stress intensity factor range, /4/. However, Damage

Tolerant Design should not be interpreted as a tool to allow continued safe operation with the known presence of a crack. This provides the required information to generate an inspection program for a component in service that would not crack under normal conditions, /5/. Infinite-life design works well for parts that are exposed to several million cycles but can be impractical for applications where excessive weight and size are factors. In most cases, the crack propagation is calculated using the Paris law, for $\Delta K > \Delta K_{th}$ /6/, also referred to as the Paris-Erdogan law, /7/:

$$da/dN = C\Delta K^m . \quad (1)$$

Out of different solutions for load configurations and standard crack geometries the users can consider the appropriate solutions to implement fracture mechanics parameters, /8/. However, there are no immediate available solutions for welded structures except for a few crack configurations /9/, as shown in Table 1. The theory of the stress intensity factor (SIF) has been developed by Irwin, as the measure of stresses in the vicinity of the crack tip /10/. The fracture toughness, K_{IC}, describes the maximum value of the material stress intensity component under plane strain conditions. Therefore, it is essential to know the crack direction and when the crack stops to propagate. The SIF is derived by a direct method or weight function method. However, the FEM calculation has been proved to be more accurate, /11-16/.

Table 1. Expressions for K_I for some geometries.

Type of crack		Stress intensity factor, K_I
Single-edge	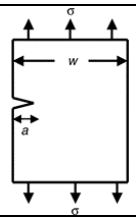	$1.12\sigma\sqrt{\pi a}$
Internal or central penny-shaped	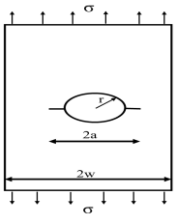	$2\sigma\sqrt{a/\pi}$
Centre crack, length 2*a*, in plate width *W*	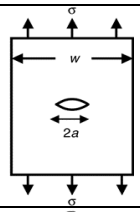	$a\sqrt{W\tan(\pi a/W)}$
Symmetrical double edge cracks, each length *a*, in a plate of total width *W*	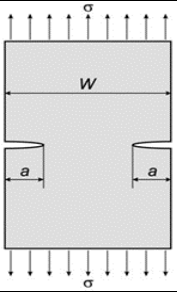	$a\sqrt{W\tan(\pi a/W)} + +0.1\sin(2\pi a/W)$

Fracture mechanics can be elasto-plastic fracture mechanics (EPFM) or linear elastic fracture mechanics (LEFM). LEFM is valid when materials demonstrate linear stress-strain behaviour. However, EPFM is an alternative mechanical approach for nonlinear material behaviour which considers parameters such as fracture criterion and crack tip condition using crack-tip opening displacement (CTOD) and J-contour integral techniques, /17/. Accuracy of several other methods concerning welding complexity is presented in Fig. 1.

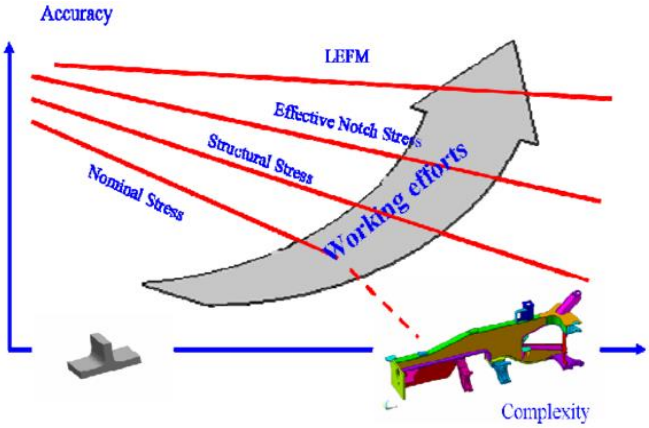

Figure 1. Relation between accuracy and complexity using various assessment methods, /18/.

Fatigue crack growth behaviour of welded steel is not reproducible. The numerical computation can give conservative probabilistic results that require fatigue crack parameters from experiments. However, residual weld stress could vanish when cutting out the conventional specimen to obtain these parameters in welded HSLA steels. The use of linear elastic fracture mechanics requires integrity, transferability, reliability and confirmability criteria together with the conventional fatigue crack growth validity and reliability evaluation criteria. The procedures for fulfilling the criteria are recommended by IIW /19/, BS7910 /20/ and many others, with differences in initial crack (defect) size, stress area and material resistance. Additionally, there is a lack of conformity in the design and deployment of welded FCG specimen, responsible for numerous variations in the design, properties, and performance of several numerical computations. Therefore, an effective test specimen is necessary to assess the FCGR efficiency of welded high strength steels. The stress-controlled high-cycle fatigue of the LEFM is defined as the eligibility criteria for this review. In this thematic review, methodological implications of investigating the efficacy of LEFM for welded high strength steel in reputable journals are discussed, and the attributes of test techniques used by different researchers in evaluation of reliable welded HSLA steel fatigue crack growth rates are examined.

BASIC PARAMETER FOR STEEL FATIGUE CRACK PROPAGATION

FCGR prediction is vital to enhance service life of steel structure which may aid decisions to evade expensive repair. At the same time, advanced reliability analysis is engaged /21, 22/. The use of established quality requirements for

decision-making is often over-conservative with permissible defects. This is why LEFM is initially developed and defined in BS7910. LEFM is capable of describing crack growth in welded structures in a physically correct way /23/. Virtually all literature agrees that the predication of FCGR by using Paris law requires the determination of pertinent parameters of the propagation curve related to properties of the material, geometry of welded joints, and calculation of the stress intensity factor range, ΔK. The stress intensity factor for large plate with a central crack is:

$$K_I = \sigma\sqrt{\pi a}\ . \tag{2}$$

A more general form of stress intensity factor is:

$$K_I = \sigma f(g)\sqrt{\pi a}\ . \tag{3}$$

The dimensionless function $f(g)$ depends on the geometry of the considered cracked body, as shown in Table 1, /23/.

To avoid a non-propagating crack, most test specimens have mechanically sharpened cracks. Crack growth is monitored with a constant or variable stress amplitude ($\Delta\sigma$), load ratio ($R = \sigma_{\min}/\sigma_{\max}$) and frequency ($\nu$), as crack length ($a$) increases with the number of fatigue cycles (N). Equation (4) summarizes the relationship among these parameters:

$$(da/dN)R,\ \nu = f(\Delta\sigma, a)\,, \tag{4}$$

where: f depends on specimen geometry and loading configuration. The FCGR test data is summarized in a plot of log da/dN vs. logΔK as shown in Fig. 2b. In Region 1, crack growth rate decreases swiftly with decreasing ΔK. It is important to note that crack growth can occur below ΔK_{th}, although it is unlikely that fatigue damage will occur at that range. ΔK_{th} for steel is typically less than 9 MPa√m /3/ and 2 MPa√m for quality weld steel when material information in not certain, /19/. This region is susceptible to changes in microstructure, environment, and mean stress, /24/. Therefore, the Paris law equation is modified to account for the difference between fatigue crack propagation threshold ΔK_{th}, and the driving force ΔK as a function of crack length as follows:

$$\frac{da}{dN} = C(\Delta K - \Delta K_{th})^m\,. \tag{5}$$

Furthermore, the relationship model between the threshold for fatigue crack propagation as a function of crack length, in this case crack length a, is measured from the free surface, as proposed by Chapetti /25/, as follows:

$$\Delta K_{th} = \Delta K_{dR} + (\Delta K_{thR} - \Delta K_{dR})[1 - e^{-k(a-d)}]. \tag{6}$$

Provided that $a \geq d$; where d is the average microstructural size (e.g. lath size, grain size etc; ΔK_{dR} is microstructural crack propagation threshold range for $a = d$; ΔK_{thR} fatigue crack propagation threshold for long cracks (dependent on R); and k is a material constant that governs transition zone shape for every stress ratio given as presented in Fig. 2a:

$$k = \Delta K_{dR}/[4d(\Delta K_{thR} - \Delta K_{dR})]. \tag{7}$$

Typically, crack growth rate in region II is linear in a log-log plot. It follows Paris' law defined by Eq.(1), where ΔK is stress intensity factor range ($K_{\max} - K_{\min}$), C and m are experimental constants, dependent on the environment, material variables, frequency, temperature, and stress ratio, /26/. Although, after the typical linear stable macroscope crack growth the next region involves accelerated crack growth, where SIF grows to its maximum value in a cycle i.e. $K_{\max}$ reaches the fracture toughness (K_{IC}) which depends on the material, temperature, strain rate, environment, and specimen geometry, /3, 27, 28/.

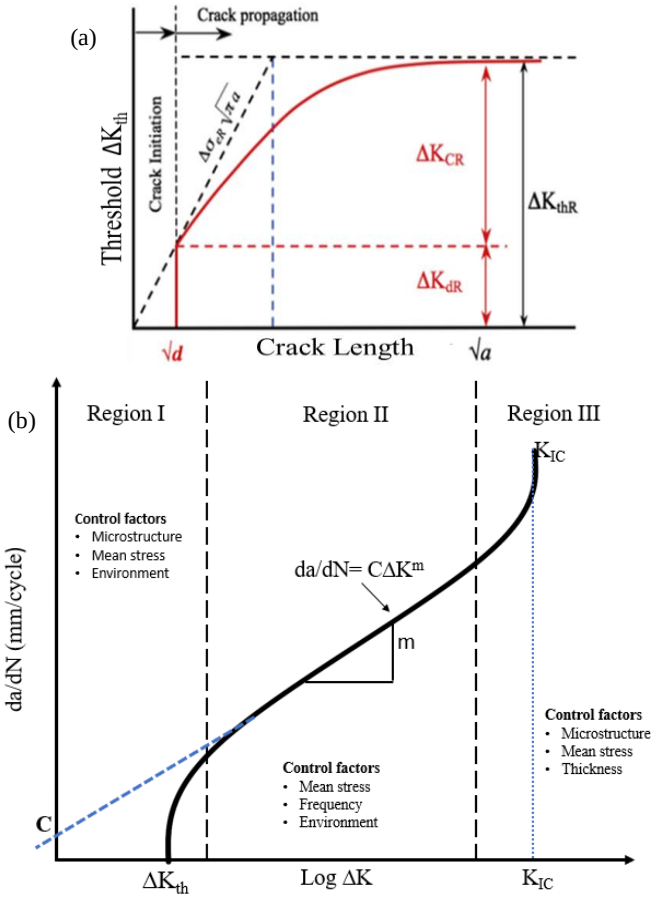

Figure 2. a) K_{th} as a function of square root of crack length, /25/; b) logda/dN vs. logΔK plot describing the three regions and influencing factors associated with crack growth rate.

For design analysis, the fracture toughness and crack length (a) are compared with failure stress σ_f:

$$\sigma_f = \frac{K_{Ic}}{\alpha\sqrt{\pi a}}\,. \tag{8}$$

The geometric parameter α is equal to 1 for specimen with edge cracks. Other crack geometries are obtainable and can be computed with finite element methods.

Fatigue fracture is based on either constant amplitude load, where the stress ratio is used along with the geometrical factor when determining $K_{\max}$ or $K_{\min}$, or variable amplitude loading which most structures and machines are subjected to in reality. Due to variability of structural loads, the Gaussian distribution does not match. Depending on application, statistical method is used to determine the root mean square of 'ΔK' /29/. So, the Paris law, Eq.(1), then becomes:

$$da/dN = C(\Delta K_{rms})^n\,. \tag{9}$$

Crack propagation at constant amplitude loading in cyclically loaded structures is rare in most practical applications /30/. However, many marine and offshore installations present a load effect interaction of the constant amplitude

loading (CAL) and variable amplitude loading (VAL), with different level of stress ratio or block- loading, which affirms that similitude cannot automatically be assumed, /31/. Mansor et al. (2019) investigated this phenomenon with X65 high strength steel for FCGR of two-level block loading by using LEFM. The transition to the high-to-low block resulted in crack growth retardation, which subsequently decreased FCGR and low-to-high loading resulted in high FCGRs /32/, as shown in Figs. 3 and 4.

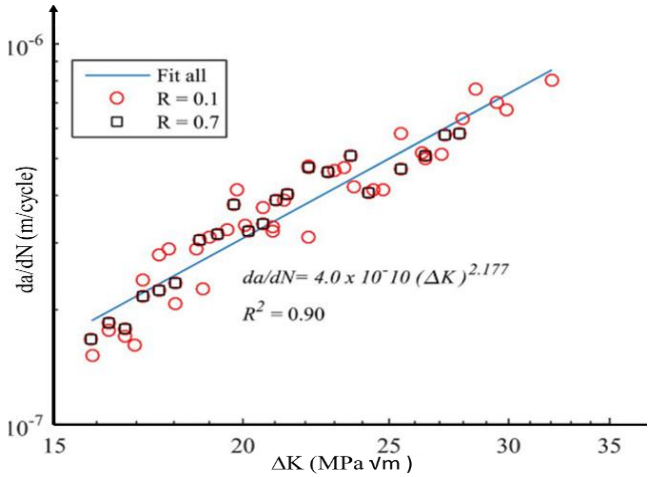

Figure 3. FCGR with fitted line for load ratios of 0.1 and 0.7.

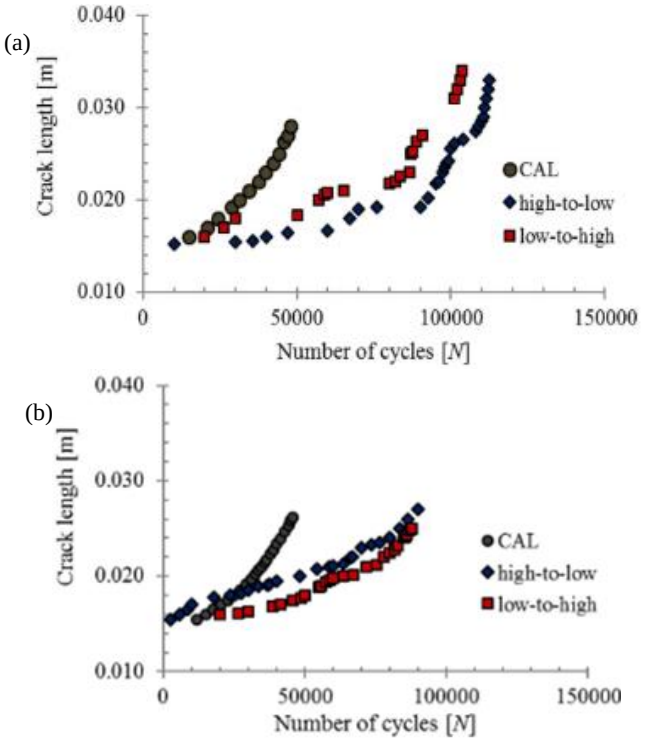

Figure 4. Comparison of fatigue crack propagation life under different loading case: CAL, high-to-low and low-to-high loading at load ratios of: a) 0.1; b) 0.7, /32/.

Maljaars et al. performed a similar experiment on welded C-Mn steel for a thin wall, although the simulated report was without the effect of residual stress, assuming residual stress is expected to remain at significant levels for larger depths. Many other efforts have supported this claim, but that of a welded high strength steel is rare.

MODELLING OF FATIGUE CRACK PROPAGATION IN WELDED HIGH STRENGTH STEEL

Estimation of stable crack growth life in the weld using fracture mechanics is basically done on two popular models. Firstly, the existence of the crack initiation phase is ignored, and the defect size of the as-welded steel crack growth calculation starts directly as recommended in IIW. Secondly, the calculation of crack growth phase with an earlier estimated number of threshold load cycle, with an initial crack length.

The desire for a more sustainable environment has influenced the continuous request for light-weight structures, with better weld strength performance, which continues to give rise to different grades of steel. High strength low alloy steels are invented for superior mechanical and corrosion properties, fatigue strength, rather than conventional carbon steels, as well as to produce adequate formability and weldability /33, 34/. Basically, high cycle fatigue is a stress-controlled phenomenon, hence, this will have higher internal energy (i.e. larger elastic region) to resist the crack /35/. Despite this advantage, weld geometry, high tensile welding stresses and early crack initiation of steels deteriorate fatigue strength of welded joints /36-/38/. Studies have confirmed that fatigue damage mostly initiates from weld notches or locations of a sudden change in the geometry and it is deemed to be the weakest link, /3, 22, 39, 40/, as demonstrated in Kitagawa diagram in Fig. 5.

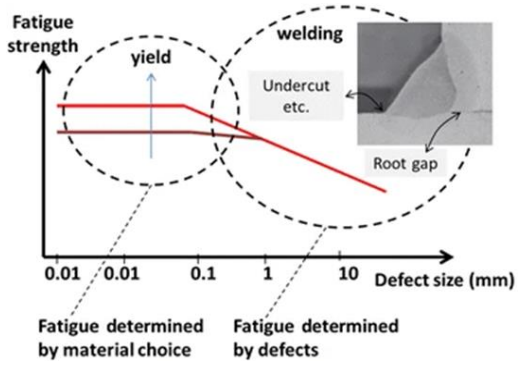

Figure 5. Kitagawa diagram, fatigue strength vs. defect size, with indicated weld positions, /41/.

Initiation and growth of the fatigue crack is dependent on the microstructural characteristics, maximum fluctuating stress and environment. The initial crack is assumed because it is still challenging to measure, in spite of the potential of fracture mechanics in fatigue evaluation of weld joint /42/.

Several analytical procedures have been proposed to estimate the fatigue crack initiation life of welds, including evaluating some of the factors affecting fatigue life and designing a model to test the initial crack size, based on BS7910 (2005). The stress intensity factor ΔK has a relationship with loading amplitude and crack size in Eq.(10),

$$\Delta K = Y \Delta\sigma \sqrt{\pi a} \ . \qquad (10)$$

Crack initiation period is regarded as when $\Delta K < \Delta K_{th}$ and crack propagates when $\Delta K > \Delta K_{th}$. The initial crack size is assumed to be a function of ΔK_{th} and stress $\Delta\sigma$, as shown in Eq.(11).

$$a = 1/\pi (\Delta K_{th} / Y \Delta\sigma)^2 . \qquad (11)$$

This academic method derives its principle from famous Kitagawa-Takahashi diagram /43, 44/. Using initial crack size of 0.1 mm, 30-40% of total fatigue life of welded joints is spent in the crack initiation phase. If the initial crack size is ≥ 0.5 mm, crack initiation life would have a more significant percentage /45/. In Zhang et al. proposed method, the initial crack size is related to loading conditions based on Eq.(3) above, it provided a definitive result and that yielded good agreement with experimental fatigue life. The applicability is validated based on the initial crack size-based procedure and took the influence of stress level into account /22/. Unfortunately, the material parameters could not determine in the expression of equivalent crack size, which is needed for more accurate prediction of total fatigue life of welded joints.

Conversely, the minimum detectable crack size, or an initial crack size recommended in standards and codes, ranges from 0.1 to 0.5 mm /46/. However, the 2014 updated version of guide for the fatigue assessment of offshore structures by the American Bureau of Shipping assumed values up to 1 mm initial crack size depending on the tubular and sheet welded steel /22, 47-50/, although Okawa et al. (2013) assumed that initial cracks are semi-circular of 0.15 mm, /51/, based on IIW recommendation, /52/. Recently, the smallest crack size detectable by X-ray inspection is 0.1 mm /53, 54/, which is consistent with the initial crack size recommended by IIW /19/. Usually, the crack detection ability decreases when the crack length direction is parallel to the magnetization direction when using non-destructive inspection. Using the proposed gradient directional magnetization system GDM, Kim et al. (2012) enhanced the crack detection capability using finite element simulations, experimental results are consistent when a crack is parallel to the scanning direction, /55/. Issues of determination of initial crack size for FCG prediction still exists due to nonconservative results /44, 56/. However, the engineering method is suitable to establish by LEFM methods, the crack propagation laws for long cracks, and then to use them also for short breaking problems. Nevertheless, when both cracks are subjected to the same value of SIF range, the short cracks can propagate appreciably faster, /57/.

In a literature survey by Kim et al. (2018), metallurgical factors influence the HCF, LCF, and FCP behaviour of high-Mn steels differently, concluded that the target service condition (i.e. the mean stress effect, temperature and environment) must be defined for developing fatigue-resistant high-Mn steels /58/. Conventionally, mean stress effects are small in region 2 while the effects can be much larger in regions 1 and 3 as seen in Fig. 2b above. Although it can cause the crack to become longer but shorten the life of welded steel component. This means that most of the loading cycles during the life of a component are during the early stages of crack growth when the crack is tiny /59/. This is expressed in Fig. 6, when stress ratio increases, crack growth rate also increases in all areas of the curve for JIS SS41 steel (ASTM A36 steel). Therefore, mean stress effects can also affect the shape of the FCGR curve /60/. The Paris equation Eq.(1) is typically modified to the Forman equation Eq.(12), /61/, to take into account stress ratio effects, /62/.

$$\frac{da}{dN} = \frac{A\Delta K^n}{(1-R)K_c - \Delta K} . \tag{12}$$

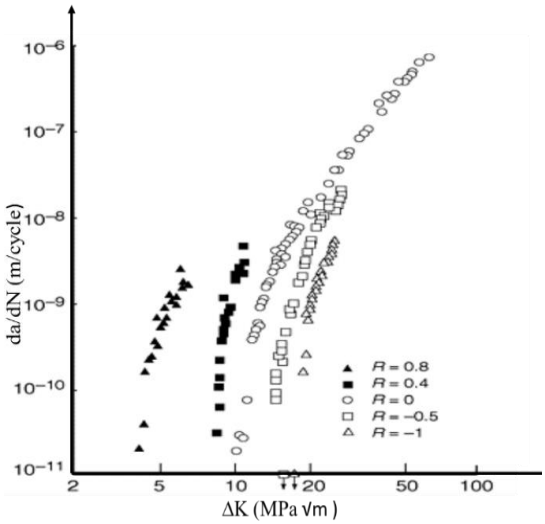

Figure 6. Comparison of load ratio (R) effects on fatigue crack growth rate in JIS SS41 steel /60/.

Since Paris law is strongly affected by mean stress R-ratio in the FCGR, residual plastic strain along the crack flanks, thereby controlling the retardation behaviour significantly /32/. Prawoto (2002) reported the necessity to predict the FCGR using LEFM with residual stresses created by the previous manufacturing process, since the total SIF driving the crack propagation is the sum of the applied SIF and the residual SIFs. The residual stresses are converted to a residual SIF using the weight function for a CT specimen, according to Eq.(13) /63/, and Fig. 7. Furthermore, the tensile residual stress will affect the stress ratio, /64/.

$$K_r = \int_0^a \sigma(x), m(a,x)dx . \tag{13}$$

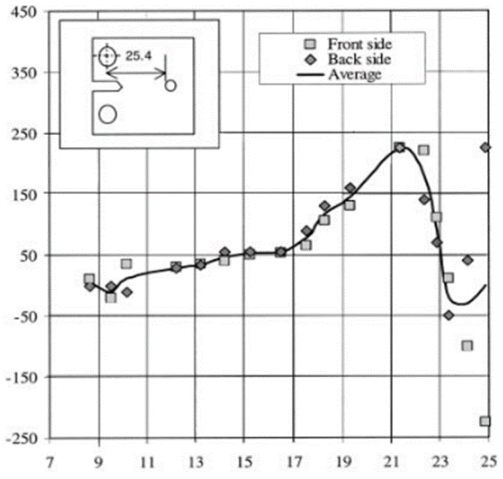

Figure 7. Initial tangential residual stress along the prospective crack line.

The possible challenge to structural integrity of the inevitable residual stresses seems to be necessary in designing lightweight welded components and structures /65/. For the analytical and numerical computation of residual stress in high cycle fatigue crack propagation, primary and secondary stress relaxation must be accounted for as the crack propa-

gates, this is not explicit in ASTM 647 yet. Nevertheless, a research project with German acronym 'IBESS' which means *Integral fracture mechanics determination of the fatigue strength of welds*, expressed for small scale yielding condition. Effective stress intensity factor of the crack front is the sum of stress intensity factor due to residual stresses K_r and stress intensity factor (K_{max} and K_{min}) due to external loading cycle, as shown in Eq.(14), /66, 67/, eliminating primary or secondary loading stress. This K_r will not affect the cyclic stress intensity ΔK, but the mean stress R-ratio.

$$R = \frac{K_{min} + K_r}{K_{max} + K_r} . \quad (14)$$

However, when residual stresses give a negative contribution to the stress intensity factor, that leads to crack closure effects, the superposition principle is not applicable based on Beghini et al. studies /66/. The principle of linear elastic ΔK loses its meaning with regards to a mechanically short crack as advised Zerbst et al. in 2018, /68/. Therefore, Hensel et al. (2018) followed the IBESS method, /69/, and the advised BS7910 published in 2005 to treat residual stresses in general as primary stresses when their extent of space is huge compared to crack size, because the elastic follow-up condition is very complicated. Hensel et al. further justify the use of stress distribution for analytical analysis in an uncracked structure and produced satisfactory results with the use of weight function methods, provided no stress relaxation when loading. This redistribution of stress during crack growth is necessary in the numerical analysis as advised by Servetti et al. in 2009 /70/, in Fig. 8. Also, Beier et al. (2015), as part of the IBESS project, could not report the redistribution caused by transient material behaviour, /71/.

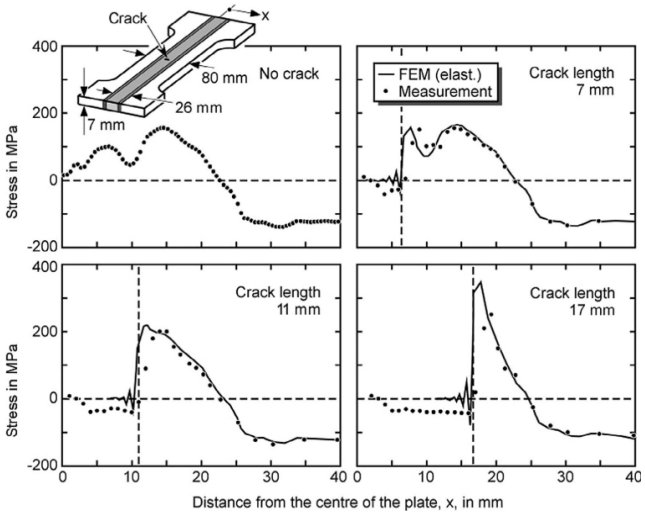

Figure 8. Redistribution of longitudinal residual stresses with crack extension.

Recall that in the design, the examined longitudinal stress is a crack opening stress /70/ and residual stresses are self-balanced making their application and measurement complex /72/. Lei et al. (2000) introduced residual stress in a finite element crack model, /73/, but similar effort is rare in the welded high strength steel. Reliance of the residual stress pattern along the weldment of high strength steel is shown in Fig. 9 /65, 67/. In the absence of restriction, the as-welded transverse residual stresses display very low values at the surface and in the thickness direction at weld toe locations and are significantly different at the weld centre-line.

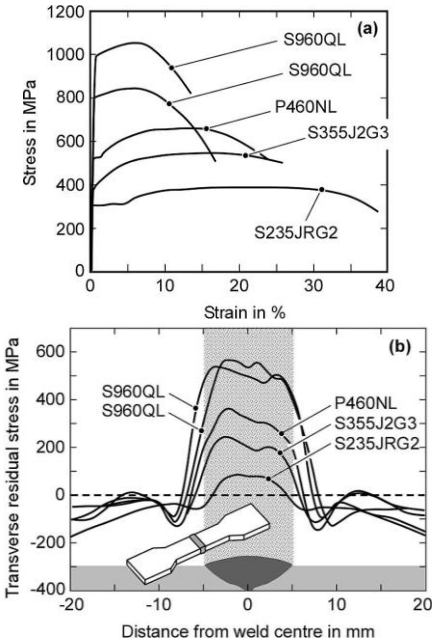

Figure 9. Transverse residual stresses at the surface of butt-welded plates: a) monotonic stress-strain curves; b) residual stress profiles at different positions including base plate, weld and weld toe, according to /65. 67/.

Furthermore, probabilistic procedures for fatigue analysis of welded steel components using the crack propagation model with numerical method are validated with experimental results /74/, however, the Paris-Erdogan equation successfully describes fatigue crack propagation with some limitation /75/. More so, correlation is developed between nonlinear and crack growth rates by using empirical and numerical equations. Critical variables for fatigue crack propagation are stress areas, material resistance and defect size, suggested by Chapetti and Steimbreger (2019) for simple fracture mechanics estimating the fatigue endurance of welded joints, /76/. This review aims to explore understanding of the effect of modelling crack growth in welded high strength steel joints, the impact of local weld notches, geometry, and reliable simulated crack predictions with threshold value for surface cracks. These tools are essential for understanding fatigue characteristics of component design, troubleshooting and predicting component failures.

FATIGUE CRACK GROWTH ON WELDED HIGH STRENGTH STRUCTURAL STEEL USING LEFM

In structural steel welding, fatigue causes approximately 60% of failures /77/, resulting in significant losses. The problem of welded structures is attributed to the difficulty to arrest fracture, the possibility of defects, the sensitivity of the material to weld, lack of reliable NDT techniques and effect of residual stress, distortion due to local heat, /78/. The fatigue life of the structure is influenced by continuous to cyclic or dynamic loading. Several years of research have analysed this phenomenon by using three primary approaches, /79/. The stress and strain based approaches centred on

the localized yield in these regions' models are too complicated to apply to engineering, and other models are only valid in some specific cases, /62, 80/. The third method is the modification of fracture mechanics for fatigue crack propagation, /81/. The Paris equation applies to the steady crack propagation zone where the length of the plastic zone ahead of the crack tip is much smaller than the crack length, /83/. The use of linear elastic fracture mechanics approach is acceptable where the data agrees with the linear relationship of log *da/dN* and log Δ*K*, /83/. However, some high strength steels exhibit elastic behaviour for small loads before plastic deformation at increased load. Therefore, it might be necessary to use elastoplastic fracture mechanics concept when the size of plastic deformation in relation to crack size cannot be neglected, hence, the parameters that take into account nonlinear plastic material behaviour, /84/. However, LEFM can predict welded fatigue life more accurately /85/. Nevertheless, the initial crack size will affect the accuracy of total fatigue life prediction /22/. Since the popular opinion is that total fatigue life is equal to crack propagation life based on existing welding defects in welded joints /86, 87/.

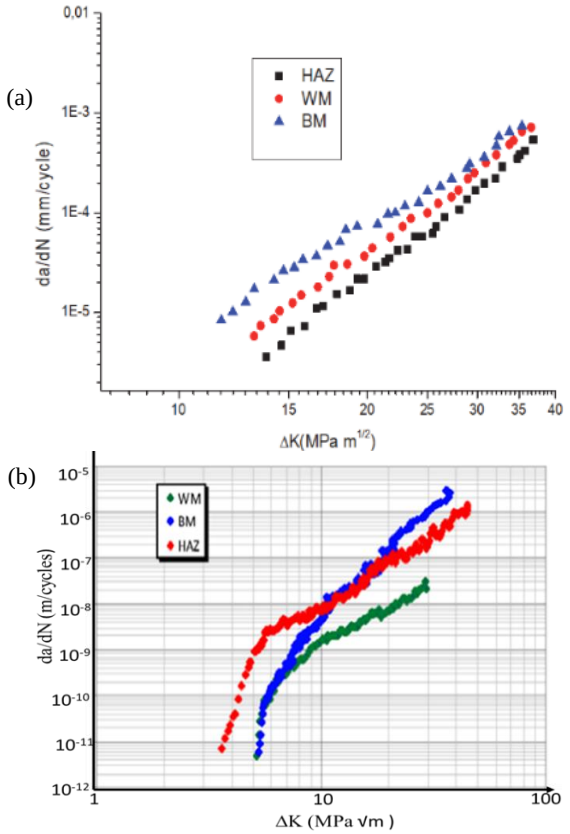

Figure 10. a) Fatigue crack growth rates vs. Δ*K* for three weld zones with CT specimen, /94/; b) Comparison of FGCR vs. SIF range for welded joint constituents with SENB specimen, /93/.

Fatigue crack parameters can only be determined at stable crack growth during crack propagation rate experiment, /50/, and depend on various influencing factors such as temperature, environmental medium post-weld treatment and loading ratio /88, 89/. Fatigue crack growth exponent *m* for steel is typically between $2 \leq m \leq 5$, /35, 90/. More so, Luke et al. (2011) findings show that the value of *m* of any steel material is independent of mean stress ratio in constant amplitude loading while the *C* is mostly dependent on the stress ratio and this always affects the threshold value ΔK_{th} /91/.

Application of LEFM with ASTM 647 test system has worked perfectly for ordinary metals, the same result might not be achieved due to welding metallurgy in high strength steel as seen in Fig. 10b, by Milović et al. (2011), where fatigue parameter ΔK_{th} value for HAZ is lower, indicating that in welded constituents, the fatigue crack will initiate first at the HAZ /92/. However, fatigue crack propagation in HAZ of welded X70 steel is delayed compared to the propagation to the other zones as reported by Deliou et al. (2018) in Fig. 10a, /93/. These inconsistencies could be attributed to the stress ratio and majorly microstructure, i.e. coarse grains of HAZ promote rapid fatigue crack growth, therefore, critical crack length and fracture strength have been reduced.

Furthermore, detailed HAZ investigation of welded HSLA steel with keen interest in the fracture mechanics parameter like thresholds and FCGR with SENB specimen of different microstructural zones of HAZ, as shown in Figs. 11 and 12 by Maier et al. (2013), since the HAZ is known as the most susceptible to crack initiation /94/. The study further presents the need for better understanding of various impact of post-weld heat treatment, machining and other manufacturing processes in the HAZ regions on the fatigue crack growth behaviour of HSLA steel, since the threshold of the base metal is low compared to the HAZ.

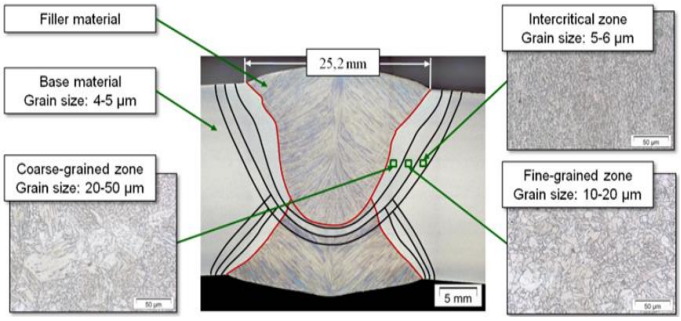

Figure 11. Microstructural zones of HAZ of a double-submerged arc welded joint.

The inter-critical zone shows disproportionately high thresholds in comparison to other zones, which the author adjudged to soft-annealing of the microstructure and leading to an increase in ductility. The normalizing effect of HAZ of welded AISI 4140 steel for different hours increased the grain size with the lowest fatigue resistance and increased FCGR as presented in Fig. 13, /95/.

In order to contribute to the development of an automatic weld process and effect of the structure on the mechanical properties and cracking resistance of arc welded joints of low-alloyed high-strength steels. The introduction of a controlled degree of irregularity to the weld toe, as a means to enhance the development and interaction of cracks and improve fatigue resistance without post-weld treatment, the double arc rotating technique (DART) is developed by Chapetti and Otegui. However, the novel method was achieved for single-pass automatic welds in thin shells, found in thin wall vessels and automotive industry with a yield strength of about 300 MPa, /96/.

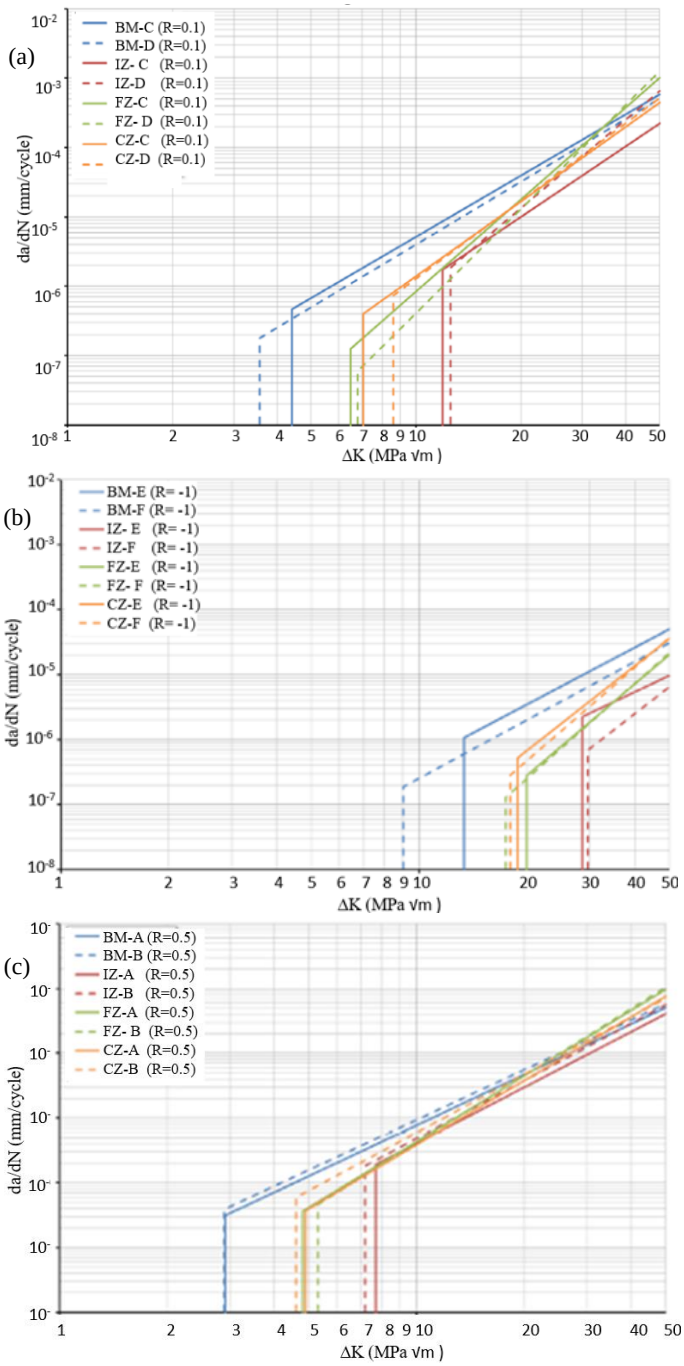

Figure 12. a) Comparison of FCG behaviour of different zones for R = 0.1; b) for R = –1; c) for R = 0.5.

Alam et al. (2005) reported the effect of weld imperfections in high strength steel with a yield strength of 390 MPa on fatigue crack propagation life. The finding shows that solidification cracks and undercuts are more serious than the embedded porosity, as shown in Fig. 14. Although the basis for an ideal weld was not described in the report. The bi-axial loading and the combined effect of a solidification crack and a circular porosity reduce the fatigue crack propagation life. Nevertheless, when they interact with each other, the fatigue life increases compared to when they are apart, /97/.

Weld geometry modification (such as grinding, re-melting, special welding techniques) removes toe defects or reduces the stress concentration and improves fatigue life and not crack propagation, /89/. The introduction of compressive stress in the area where cracks are likely to initiate (such as mechanical peening/overloading) /98/ are the established weld improvement methods. Hence thermal PWHT is not advised for HSLA steel. However, when multiple notched welds are present, post-weld impact treatment will be necessary. High frequency mechanical impact (HFMI) method has proved some favourable results from literature /9, 99-102/. Nevertheless, the authors emphasize that minimum and maximum stress, and not merely the stress range, has a significant influence on the observed degree of fatigue improvement, /99/.

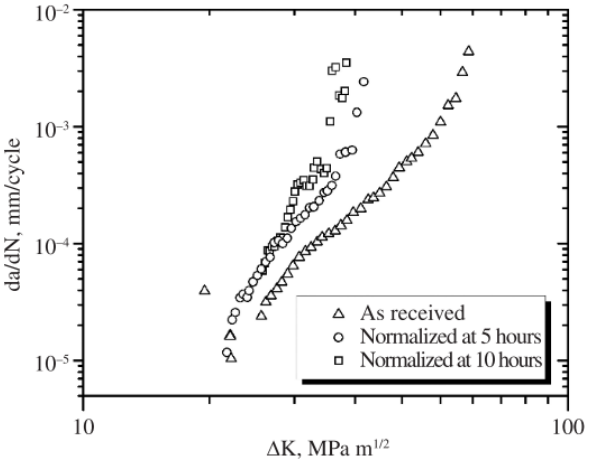

Figure 13. Plot of crack growth rate behaviour with SIF for HAZ normalized at 1200°C for different time, /95/.

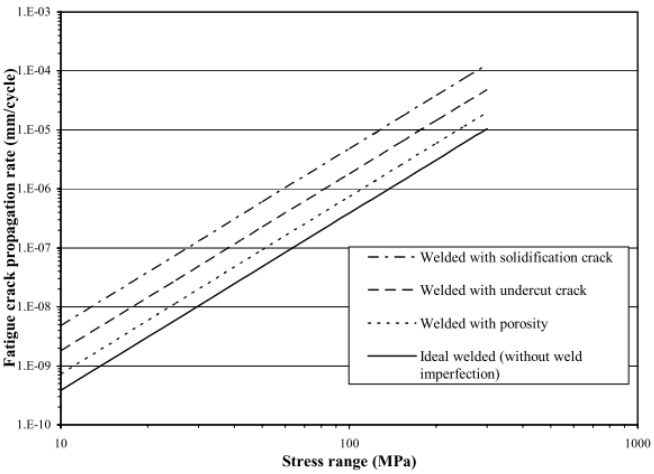

Figure 14. Effect of weld imperfections on the fatigue crack propagation rate, /97/.

The influence of welding consumables was explored to improve the FCGR of weld QT grade armour steel, finding that the FCG resistance of SMAW is better than that of FCAW, regardless of consumables. However, low hydrogen ferritic steel consumables provided enhanced FCG resistance due to beneficial residual stress based on fracture mechanics /35, 103, 105/. Furthermore, mismatch ratio is inversely proportional to the FCG exponent m and is directly proportional to the threshold stress intensity factor K_{th}, and critical stress intensity factor which boost fatigue performance of HSLA steel over the joints, /105/. However, an approach

based on different combinations of mainly Ni and Cr to produce low martensite-start (M_s) temperatures of welding filler wire capable of inducing a local compressive residual stress using *low transformation temperature* (LTT) consumables is favourable based on several literature findings /106-110/. The FCGR of conventional and LTT wire filler for welded steel, reported by Ohta et al., is shown in Fig. 15 /111/.

Nevertheless, Lukas and Dobosy (2019) acknowledged that the weld consumable mismatch and orientation of FCG specimens, within the same material strength category and production condition (QT and TM), caused a major variation in the parameters for fatigue crack growth resistance, as stated in Table 2, /113/. Conversely, the fatigue crack threshold was not reported.

Recently, Otterbuck et al. (2019) considered initial crack phase for LEFM investigation using SENT specimen. The initial crack size was determined by the number of cycles to crack initiation, and optical detection procedure for undercut. Three different sets of welded crack propagation parameters for the Paris law were reported, as seen in Table 2. In the report, actual fracture fatigue life test is observed with digital image correlation principle with digital single-lens reflex (SLR) camera system, and the best fit parameter methodology is more conservative, /113/. The improved component design, troubleshooting and prediction is made by introducing a new SENT specimen. Even though the SENT was developed to reduce the complexity effort required for crack propagation problems, none of the studies compare efficiency with the conventional specimen.

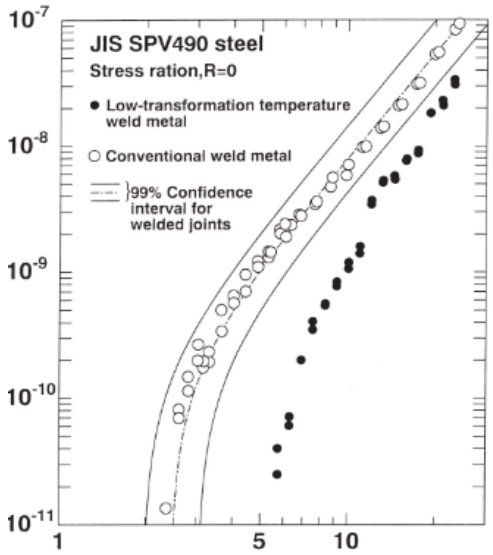

Figure 15. Comparison of fatigue crack growth properties of welded joints produced with conventional and LTT welding consumables, /111/, improvement of high strength steel weld.

Finally, as Table 2 demonstrates, some methodology of FCG evaluation of welded HSS is consistently better than the other with the same LEFM approach. Hence, the principal assessment of FCGR of welded high strength steel remains the comparison of the effective crack driving force in welded high strength steels using the methodology that incorporates the attributes articulated in IIW recommendation and the best fit parameters resulting by a least square fit of the fatigue test results.

Table 2. Characteristics of fatigue crack growth of welded high strength steel with linear elastic fracture mechanics based.

Author	**Material/ yield strength/ thickness**	**Post weld**	**Test specimen**	**Stress ratio (*R*)**	***C***	***m***	**ΔK_{th} (MPa√m)**	**K_{IC} (MPa√m)**	**Initial crack size**	**Consumables**	**Crack measuring system**	**Type of weld**
					Based on specimen orientation with respect to the weld axis/zone for FCG							
Ravi et al. 2004 /105/	HSLA-80 /12 mm		CCT	0	UM:7.33e^{-10} M: 1.04e^{-09} OM:1.59e^{-09}	4.20 3.85 3.43	5.5 6.0 6.5	25 35 45	8 mm crack at weld centre-line	E8018G E11018M E13018G (low-H ferrite electrode)	traveling microscope	not stated
Milović et al. 2011 /93/	HSLA (700MPa)/ 18 mm	overfill grinding	SENB	0	BM:9.05e^{-14} HAZ:8.06e^{-12} WM:6.07e^{-12}	4.76 3.054 2.393	5.85 4.3 5.82	no data	1.029 mm	not incorporated	Strain gauge causing linear electrical resistance response	
Maier et al 2013 /94/	HSLA/ 20 mm		SENB	0.5	determined for every zone of HAZ	determined for every zone of HAZ	HAZ CZ, IZ, FZ 4.90, 7.70, 4.80 4.60, 7.20, 5.30	no data		not incorporated	In-house developed direct-current potential-drop (DCPD) measurement system magnification stereoscope tracing a set of reference marks and crack length measurement from machine software	Double submerged arc welding (SAW) with high $t_{8/5}$ times. Gleeble thermal simulator made similar micro-structural specimen
				0.1	determined for every zone of HAZ	determined for every zone of HAZ	HAZ CZ, IZ, FZ 7.05, 11.90, 6.50 8.60, 12.55, 6.80					
				-0.1	determined for every zone of HAZ	determined for every zone of HAZ	HAZ CZ, IZ, FZ 18.84, 28.50, 19.98 18.00, 29.65, 17.50					

Vargas-Arista, et al. 2013 /95/	4140 steel/ 710 MPa/ 18 mm	HAZ was normalized at 1200 C	SENB	0.1					7.8 mm	AWS E7018		SMAW
Mecseri et al. 2017 /89/	S420 HSLA/ 10 mm	disc grinding			$8.31e-13$	3.03			Flange gusset joint		Electrical potential difference (EPD) method and Visual crack measuring	
		No grinding			$1.50e-12$	2.92						
Deliou et al. 2018 /93/	API 5L X70 grade/ 500.3 MPa /7 mm		CT	0.1	not defined	not defined	not defined			C_{eq} contents of BM and WM calculated with IIW proposal are resp. 0.36% and 0.39%	Evolution of crack length according to the number of cycles	Submerged arc welding
Lukács and Dobosy 2019 /112/	S700 / 801 MPa/ 13 mm		SENB	0.1	T-L, L-T: $8.09e-07$	1.7	not determined	101		Base material	Stereo microscope (optical method, using video camera, hundred-fold magnification (N = ×100)	GMAW
					T-S $2.06e-06$	1.50		75	Initial crack on the centre-line on weld joint	Union X85 T filler wire (M)		
					21W: $1.12e-11$	4.10		105				
					23W: $4.93e-08$	2.30		80		Union X90 T filler wire (OM)		
					21W: $4.02e-07$	1.85		96				
					23W: $3.19e-07$	1.90		61				
	S960Q (Q&T)/ 1030MPa / 13mm				T-S, L-S, T-L: $3.50e-07$	1.80		94		Base material		
					21W & 23W: $1.03e-08$	2.75		93		Union X96 T filler wire (M)		
	S960M (TM)/ 1051MPa / 13mm				T-L, L-T: $4.63e-07$	1.82		116		Base material		
					T-S: $6.41e-07$	1.75		87				
					21W: $3.19e-07$	1.90		114		Union X96 T filler wire (M)		
					23W: $6.06e-09$	2.75		82				
					21W: $3.10e-08$	2.40		115		Turboid 14.03 filler wire (UM)		
					23W: $9.93e-08$	2.15		67				
Ottersböck et al. 2019 /113/	Ultra high strength steel / ≥1100 / 6 mm		SENT	0.1	8.35e-10	1.72			$*a_i$ = 0.5mm + N^{th} cycle	T89 metal core filler wire	S1100 base material property	not incor-porated
					8.35e-10	1.72			$**a_i$ = U + 0.1mm			
					5.21e-13	3.0			$*a_i$ = 0.5mm + N^{th} cycle	T89 metal core filler wire	suggested IIW parameters for welds	
					5.21e-13	3.0			$**a_i$ = U + 0.1mm			
					1.78e-13	2.90			$*a_i$ = 0.5mm + N^{th} cycle	T89 metal core filler wire	(Best fit parameters resulting by a least square fit of the fatigue test results)	
					1.00e-13	2.85			$**a_i$ = U + 0.1mm			
Cabrillo et al. 2019 /103/	Armour steel/ 1205/ 12 mm		SENB	not stated	BM: $1.0e-09$ HAZ: $6.0e-13$ WM: $1.0e-12$	BM: 3.35 HAZ: 5.97 WM: 5.10	BM: 13.4 HAZ: 15.2 WM: 10.1	861 286 355	5 mm for all specimen region	AWS ER307	analysis of fracture surface carried out after exami-nation of fatigue crack growth rate	GMAW

$*a_i$ = 0.5 mm + N^{th} cycle; start of calculation at the previously determined threshold load cycle number (N^{th}) with an initial crack length.
$**a_i$ = U + 0.1 mm; calculation from the test start with an initial crack length, i.e. detected undercut (U) as recommended in IIW /19/.
OM-overmatching welding; M-matching welding; UM-undermatching welding; T-transverse; L-longitudinal; S-short; W-width; *m*-Paris-Erdogan exponents; *C*-crack intercept

Apart from the methodology issues, the use of small-scale specimens for FGCR testing is a concern as it relates to the issue of full-scale effect in fracture mechanics. However, if measuring FCG below a critical threshold, the specimen thickness is not a significant parameter in fracture /89, 114/, validated by Li and Stubbins (2002) with 2 mm thickness SENB notch bar specimens that produced similar crack growth behaviour to that of standard specimens (CT) for three materials in yield strength, ranging from 300 to 1200 MPa. Reliable crack growth data for *a/W* of 0.5 covering the full Paris law crack growth regime could be obtained, /115, 116/. The ASTM-E647 standard placed strict requirements on the size of conventional specimens (e.g. $W \geq 25$ mm, $W/20 \leq B \leq W/4$; for C(T) specimen) and hence, a large amount of material is needed to fabricate the specimens, also for the evaluation of various mechanical properties, /115/. Therefore, Chauhan et al. (2016) engaged miniature Single Edge Notched Tensile (SENT) specimens to study FGCR and to obtain material constants of (20MnMo Ni55) steel according to ASTM-E647 standard of same order as the conventional specimen within the same stress intensity and FCGR /91/. A suitable specimen in the shape of modified SE(T) was used to analyse variable amplitude crack growth in both experimental tests, and predictive models of A1N steel grade exhibited favourable results compared to traditional SE(B) specimen in rail axle application using fracture mechanic approach /117/. Furthermore, measuring effects of the strain/crack gauges are analysed, the stresses near the crack decreases as the crack progresses, but the stresses on the other side increase, since the direction of crack propagation is always perpendicular to the edge of the base plate, and the path of the stress lines vary close to the fatigue crack in SENT specimen, as presented in Fig. 16, /89/.

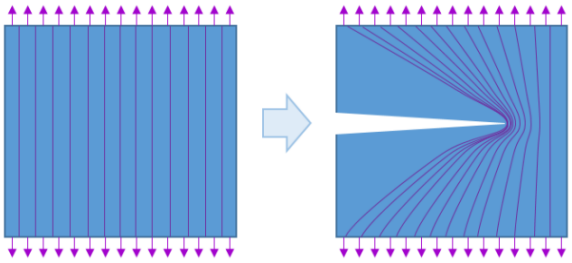

Figure 16. Change of stress field due to crack propagation.

A better understanding of the constraint effects on fracture toughness is imperative to bring the small specimen methodologies under the ambit of standards and codes for its acceptance. Integration of small specimen tests with numerical analysis and fracture models together with microstructural analysis is the way forward. To compensate for crack tip constraint effects, ISO 27306: 2016 proposed two methods. First one is to correct the numerical difference in constraint between the test and actual configuration (i.e. converting the CTOD fracture toughness obtained from laboratory specimens to an equivalent CTOD for structural components, taking constraint loss into account). This method can also be applied to fracture assessment using the stress intensity factor, /118/. The second method is to use a specimen configuration that represents the intended application.

Results from this review show that the probable intervention to form an equiaxial grain fine-grained bainite-martensitic structure in welded joints could have substantial benefit, which is achieved by reducing the heat input in welding to values below 500 J/mm, as characteristic for laser and hybrid laser-arc welding /119/. However, in welded components of high strength steel, the fatigue strength will be the same for mild steel if no improvement of weld quality is achieved /41/. The loss of constraint is significant for high strength steels with high yield-to-tensile ratios which motivated the development of this single edge notch tension (SENT) testing procedure /120, 121/. The development of SENT specimens has been widely accepted within the oil and gas industry as this specimen best represents a shallow surface-breaking crack subjected to a tensile load /122, 123/. The SENT specimen may eliminate the loss of residual stresses due to machining. Conversely, a general standardized procedure is unknown to use SENT specimen for FCGR.

MODELLING AND SIMULATION OF FCG ON WELDED HIGH STRENGTH STEEL

In studies included in this review, researchers have explored fatigue crack propagation of welded high strength steel with LEFM, using different numerical models. LEFM captures practical crack growth, conversely at much more computational time /124/. However, the effect of weld process - residual stresses in high strength steel makes it challenging to deploy FCGR numerical model, leading to many efforts to simplify fatigue test model with tensile residual stresses. However, the reliability of their results is limited /125/ since welding simulation requires calibration. FEM is a robust method developed for many engineering applications. Despite these advantages, the FEM requires grid generation methods to discretize the solution domain /126, 127/. Compared to BEM, FEM has more computational costs. Effective grid algorithms and FEM solvers could decrease computational costs /128, 129/. FEM is perhaps the most common method of obtaining stress intensity and FCG. Two main emerging concepts of FEM are the fractal and extended method. Despite FEM versatility, a coupled process of welding high strength steel and FCGR with FEM is rarely available.

Underlying assumption and criteria for the simulation model is such that, in one external load cycle, the crack front goes through a micro-mechanism involving crack blunting and re-sharpening as stress rises and decreases /130/, with other growth parameters like increment steps, total number of steps, growth model, etc. Yang et al. (2017) incorporated LEFM based algorithm for 3D fatigue crack growth simulation for both cyclic and torsion loading with finite element program ABAQUS and fracture analysis software FRANC 3D, as shown in Fig. 17 with HSS S460N material mechanical properties. Although experimental validation agrees with the aluminium specimen, the steel specimen FCGR was faster than the predicted results in both loading conditions /131/, as seen in Fig. 18.

Several crack initiation sites from the weld toe are common features in welds, however, this crack initiation depends on the variations of local geometry and load rates

/132/. Dong and Soares (2018) predicted SIF of semi-elliptical surface crack originating from tip of the weld toes with weight function approach using Baik et al. /133/ experiment results for FEM re-analysis. The LEFM crack propagation analysis is determined based on BS7910 recommended material constant. Also, Gahfoori et al. (2018) examined the SIF calculation of crack under tensile load by analytical calculation and numerical approach, the accuracy of crack length was not affected in both approaches, except where the mesh size ratio was high for the numerical simulation /134/. Conversely, fine meshing with more computational time will give the most accurate prediction, /135/.

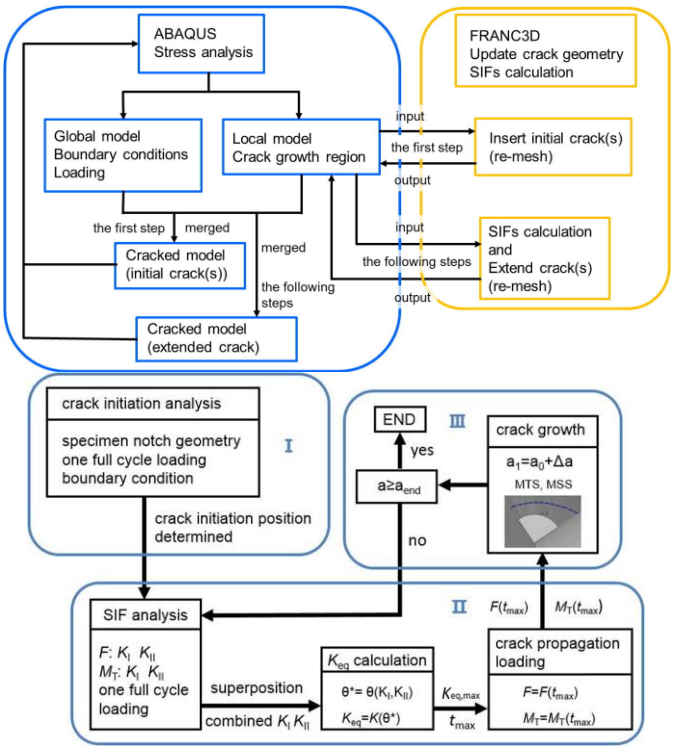

Figure 17. ABAQUS/FRANC 3D working flow and simulation algorithm, /131/.

Theoretically, when the local parameters near the crack tip can be observed through high resolution techniques, the type of crack behaviour is eliminated /57/. Therefore, Stenberg et al. (2019) developed and examined the computation algorithm fatigue strength of welded of S355 and S960 by direct measurement of weld imperfection in geometry using a surrogate model in Fig. 21, A crack is remodelled at the maximum principal stress position in the previous region and stress intensity factor ΔK_I is solved using the same approach with load cases superimposed as shown in Fig. 22. The second segment of study used the algorithm over a set of prescribed crack depths to determine ΔK_I as a discretized function of crack depth a, which calibrates stress intensity factor against an analytical solution with similar characteristics. With mesh size consideration, the initial crack size precision of experimental fatigue life and the computed is virtually zero /139/.

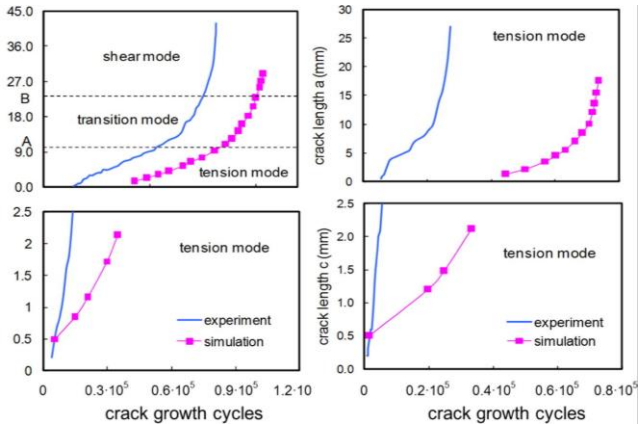

Figure 18. Steel crack growth curve for two specimens /131/.

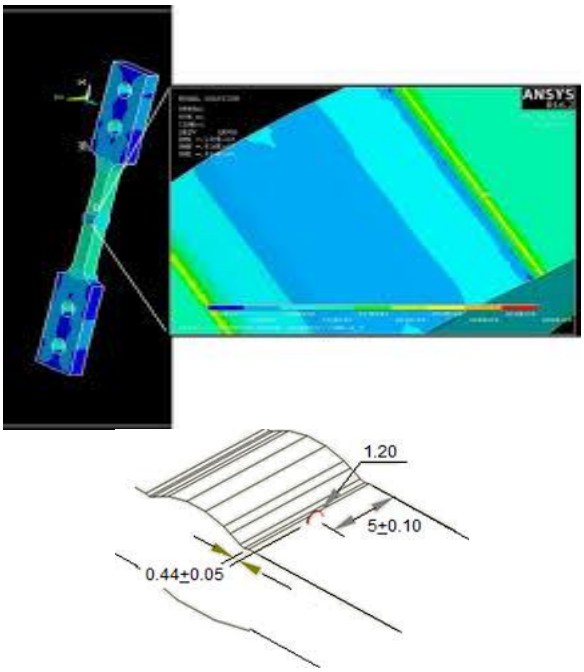

Figure 19. a) Stress distribution (von Mises); b) location of the flaw in welding, /138/.

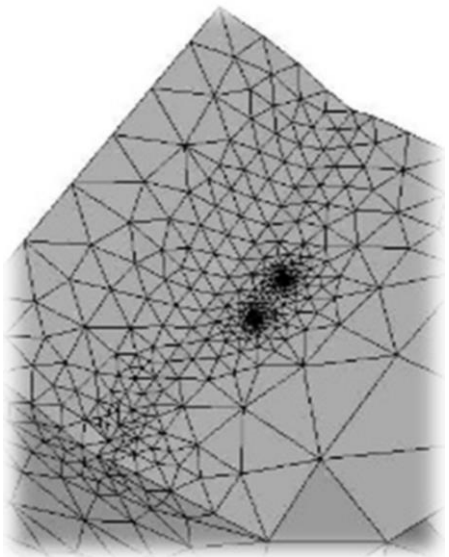

Figure 20. Crack inserted in the model (FRANC 3D), /138/.

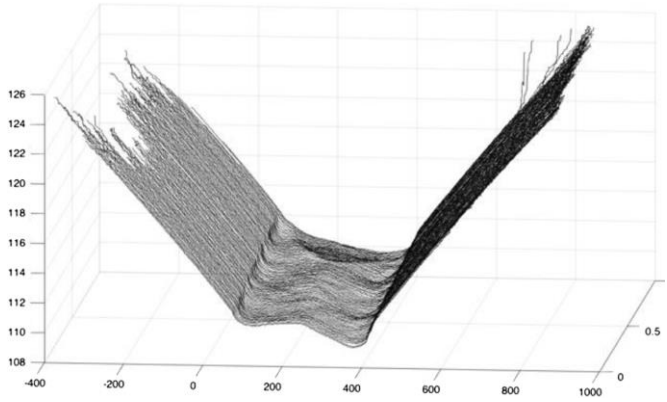

Figure 21. Weld geometry representation with discretized cross sections, /139/.

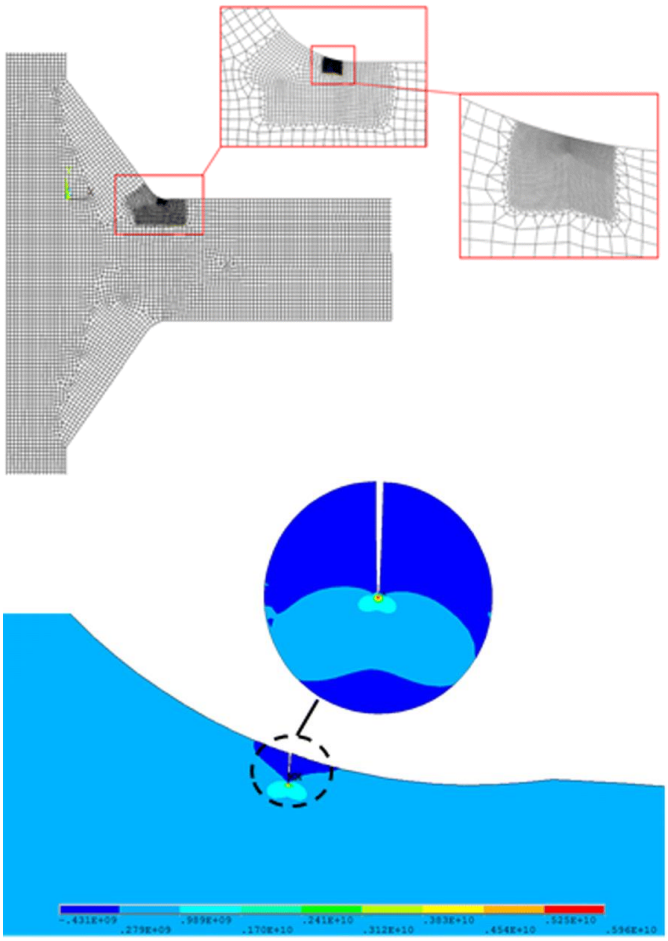

Figure 22. FE fracture mechanical model, /139/.

However, the developed model has not yet satisfied linear elastic fracture mechanics for thin plate, so the study concludes that since the crack length is too large in comparison to the thickness of the specimens, the plastic zone near the crack may be relatively large compared to the dimensions of the load carrying area at the weld. Nevertheless, computational analysis of reinforcement size in FCGR reveals that bead reinforcement is proportional to the concentration of local stress in the crack tip by no major plastic deformations, which is why the material elastic range is adequate to clarify the stress behaviour of the specimen with the Paris model, /138/.

In the literature reviewed, the need to improve and understand procedure for numerical estimation of fatigue crack propagation rate in welded high strength steel is articulated, to prevent highly complicated, expensive and time consuming joint geometry, the amount of stress concentration points and the heterogeneous weld metal properties of the joint.

CONCLUSION

Experimental and numerical LEFM can provide reasonable predictions for the fatigue crack growth propagation in welded high strength steel. Determination of FCGR process parameters from experiments requires FEM approach to complement the accurate determination of SIF, initial crack size, residual stress along the crack plane, etc. Therefore, focus on applying and improving these techniques to solve complex problems in conformity with the relevant standard is required. Among them, the following seems to be of particular interest:

– Since the initial crack size plays an essential role in the analysis of fatigue crack propagation, FEM approach using LEFM can predict welded fatigue life more accurately, and the popular opinion is that total fatigue life is equal to crack propagation life based on existing welding defects in welded joints.
– A note of caution suggests that, if near-threshold data generated from long cracks are used to predict the life of components containing short cracks, non-conservative estimates may result.
– Conventionally, the fatigue crack growth rate of steel was thought to show little sensitivity to the microstructure, but welded high strength steel with different grain size in different zones show a distinct influence on FCGR. However, discrepancies still exist within the same weld region.
– Several relationships of LEFM prediction method and the influencing factors have been proposed.
– Measuring ΔK_{th} values for base materials and welded joints, stress concentration at a given depth from the fatigue crack initiation point, given by the macro-geometry of the welded joint, is still not explored for validity, hence, requires additional effort.
– PWHT does not improve the fatigue crack growth rate of welded high strength steel. However, post-weld mechanical treatment, such as HFMI/PIT, shows some level of improvement.
– Under linear elastic fracture mechanics conditions, local re-meshing is necessary in advance of the crack in FEM to complement the SIF. Nevertheless, FEM simulations in loading interaction effect FCGR in most of the application of high strength steel is rare.
– Although FEM has found application in almost all areas of nonlinear and fracture mechanics, still there are challenges in developing computationally efficient algorithms with accurate meshing techniques with scalable implementation of coupled welded and FCGR simulation.
– Residual stresses are self-balancing, weld residual stress could vanish when cutting out the conventional specimen, hence, single edge notch tension (SENT) is expected to eliminate this phenomenon when measuring the FCGR in high strength steel welds.

The ability to understand and predict fatigue crack growth in welded high strength steel is essential in design, and safe continuous operation is very complex due to residual effect, grain size, loading sequences, weld defect, environment. Most of the FEM simulation in the literature do not include any corrections for residual stresses by coupling welding and FGCR for high strength steel in recent literature.

FURTHER RECOMMENDATIONS

Differences between FCGR test specimen of welded high strength steel account for some variability in the test results. Therefore, a uniform standard on a welded high strength steel test specimen that incorporates attributes articulated in this review is highly needed to ensure comparison. This measure will help establish adequate specimen that could be used to validate numerical computation such as the finite element method to generate reliable weld structural integrity outcomes in linear elastic fracture mechanics. It is expected that this information will be valuable to product developers, other researchers seeking to improve or optimize high strength steel welding for fatigue strength and avoidance of destructive test accompanied with high costs.

In FEM, the consideration of the inherent property due to welded high strength steel for evaluating the stress intensity factors is seldom engaged. For both analysis methods, there is also a focus on improving their efficiency by introducing new SENT specimen. Even though the SENT is developed to reduce the complexity effort required for crack propagation problems, none of the studies reviewed do compare efficiency between conventional specimen. Likewise, simulation of welding and cracks, with SENT considering residual stress. Significantly, there is room for many possible developments and improvements.

REFERENCES

1. Sapora, A., Cornetti, P., Campagnolo, A., Meneghetti, G. (2020), *Fatigue limit: Crack and notch sensitivity by finite fracture mechanics*, Theor. Appl. Fract. Mech. 105: 1-6. doi: 10.1016/j.tafmec.2019.102407
2. Kliman, V., Chmelko, V., Margetin, M. (2015), *Analysis of the notch effect of welded joint and of grinding effect*, Kov. Mater. 53(6): 429-441. doi: 10.4149/km_2015_6_429
3. Stephens, R.I., Fatemi, A., Stephens, R.R., Fuchs, H.O., Metal Fatigue in Engineering, 2nd Ed., Wiley, 2000.
4. DeMarte, R.A., Analysis of Fatigue Crack Propagation in Welded Steels, M.Sc. Thesis, Marquette University, Milwaukee, Wisconsin, USA, 2016.
5. ASM Handbook Vol.11: Failure Analysis and Prevention, ASM Int., Mater. Park, OH, USA: 227-242; 559-586, 2002. doi: 10.31399/asm.hb.v11.9781627082952
6. Paris, P., Erdogan, F. (1963), *A critical analysis of crack propagation laws*, J Basic Eng. 85(4): 528-534. doi: 10.1115/1.3656 900
7. Fuštar, B., Lukačević, I., Dujmović, D. (2018), *Review of fatigue assessment methods for welded steel structures*, Adv. Civ. Eng. 2018(9): 1-16. doi: 10.1155/2018/3597356
8. Al Laham, S., Stress Intensity Factor and Limit Load Handbook, SINTAP/Task 2.6, EPD/GEN/REP/0316/98 (issue 2), British Energy Gen. Ltd., 1999.
9. Leitner, M., Barsoum, Z., Schäfers, F. (2016), *Crack propagation analysis and rehabilitation by HFMI of pre-fatigued welded structures*, Weld. World, 60(3): 581-592. doi: 10.1007/s40194-016-0316-x
10. Irwin, G.R. (1957), *Analysis of stresses and strains near the end of a crack traversing a plate*, J Appl. Mech. ASME, 24: 361-364.
11. Bao, R., Zhang, X., Yahaya, N.A. (2010), *Evaluating stress intensity factors due to weld residual stresses by the weight function and finite element methods*, Eng. Fract. Mech. 77(13): 2550-2566. doi: 10.1016/j.engfracmech.2010.06.002
12. Caicedo, J., Portela, A. (2017), *Direct computation of stress intensity factors in finite element method*, Eur. J Comput. Mech. 26(3): 309-335. doi: 10.1080/17797179.2017.1354578
13. Xiao, Q.Z., Karihaloo, B.L. (2004), *Evaluation of higher order weight functions by the finite element method*, In: Proc. 15th Europ. Conf. on Fracture (ECF 15), F. Nilsson (Ed.), Stockholm, Sweden, 2004.
14. Gupta, P., Duarte, C.A., Dhankhar, A. (2017), *Accuracy and robustness of stress intensity factor extraction methods for the generalized/eXtended Finite Element Method*, Eng. Fract. Mech. 179: 120-153. doi: 10.1016/j.engfracmech.2017.03.035
15. Ramesh, K., Gupta, S., Kelkar, A.A. (1997), *Evaluation of stress field parameters in fracture mechanics by photoelasticity-revisited*, Eng. Fract. Mech. 56(1): 25-41, 43-45. doi: 10.1016/S0013-7944(96)00098-7
16. Al-Mukhtar, A., Biermann, H., Henkel, S., Hübner, P. (2010), *Comparison of the stress intensity factor of load-carrying cruciform welded joints with different geometries*, J Mater. Eng. Perform. 19: 802-809. doi: 10.1007/s11665-009-9552-1
17. Anderson, T.L., Fracture Mechanics: Fundamentals and Applications, 3rd Ed., CRC Press, 2005. doi: 10.1201/9781420058215
18. Barsoum, T.L., Residual Stress Analysis and Fatigue Assessment of Welded Steel Structures, Doctoral Thesis, School of Eng. Sci., Kungliga Tekniska Högskolan (KTH), Stockholm, Sweden, 2008.
19. Hobbacher, A.F., Recommendations for Fatigue Design of Welded Joints and Components, Springer Int. Publ., 2016. doi: 10.1007/978-3-319-23757-2
20. BS 7910:2005, Guide to methods for assessing the acceptability of flaws in metallic structures (incl. A1, 2007), 2005.
21. Al-Mukhtar, A.M., Biermann, H., Hübner, P., Henkel, S. (2010), *Determination of some parameters for fatigue life in welded joints using fracture mechanics method*, J Mater. Eng. Perform. 19(9): 1225-1234. doi: 10.1007/s11665-010-9621-5
22. Zhang, X., Gao, H., Huang, H.Z. (2018), *Total fatigue life prediction for welded joints based on initial and equivalent crack size determination*, Int. J Damage Mech. 27(7): 1084-1104. doi: 10.1177/1056789517723171
23. Alam, M.M., et al. (2009), *Fatigue behaviour study of laser hybrid welded eccentric fillet joints - Part II: State-of-the-art of fracture mechanics and fatigue analysis of welded joints*, In: 12th NOLAMP Proc. 2009: Nordic Laser Mater. Proces. Conf., E.D. Mortensen (Ed.), Copenhagen, Denmark, 2009, pp.1-33.
24. Martelo, D.F., Chapetti, M.D. (2015), *Analysis of the importance of the crack closure in the driving force for the fatigue crack growth in metastable austenitic stainless steels*, Procedia Mater. Sci. 9: 387-395. doi: 10.1016/j.mspro.2015.05.008
25. Chapetti, M.D. (2003), *Fatigue propagation threshold of short cracks under constant amplitude loading*, Int. J Fatigue, 25(12): 1319-1326. doi: 10.1016/S0142-1123(03)00065-3
26. ASM Handbook, Vol.19: Fatigue and Fracture, ASM Int., Mater. Park. OH, USA: 15-26, 63-72, 1996. doi: 10.31399/asm.hb.v19.9781627081931
27. Lassen, T., Récho, N., Fatigue Life Analyses of Welded Structures: Flaws, Wiley-ISTE, 2010.
28. Darcis, P., Santarosa, D., Récho, N., T. Lassen (2004), *A fracture mechanics approach for the crack growth in welded joints with reference to BS 7910*, In: Proc. 15th Europ. Conf. on Fracture (ECF 15), F. Nilsson (Ed.), Stockholm, Sweden, 2004.

29. Vikram, N., Kumar, R. (2013), *Review on fatigue-crack growth and finite element method*, Int. J Sci. Eng. Res. 4(4): 833-843.
30. Simunek, D., Leitner, M., Maierhofer, J., Gänser, H.P. (2015), *Fatigue crack growth under constant and variable amplitude loading at semi-elliptical and V-notched steel specimens*, Procedia Eng. 133: 348-361. doi: 10.1016/j.proeng.2015.12.670
31. Jones Ac, R., Chen, B., Pitt, S. (2007), *Similitude: Fatigue cracking in steels*, Theor. Appl. Fract. Mech. 48(2): 161-168. doi: 10.1016/j.tafmec.2007.05.007
32. Mansor, N.I.I., Abdullah, S., Ariffin, A.K. (2019), *Effect of loading sequences on fatigue crack growth and crack closure in API X65 steel*, Mar. Struct. 65: 181-196. doi: 10.1016/j.marstruc.2019.01.007
33. ASM Int., Alloying: Understanding the Basics, J.R. Davis (Ed.), Materials Park, OH, USA, 2001.
34. Beretta, S., Carboni, M., Cantini, S., Ghidini, A. (2004), *Application of fatigue crack growth algorithms to railway axles and comparison of two steel grades*, Proc. Inst. Mech. Eng., Part F: J Rail Rapid Transit, 218(4): 317-326. doi: 10.1243/0954409043125888
35. Magudeeswaran, G., Balasubramanian, V., Madhusudhan Reddy, G. (2014), *Effect of welding processes and consumables on fatigue crack growth behaviour of armour grade quenched and tempered steel joints*, Def. Technol. 10(1): 47-59. doi: 10.1016/j.dt.2014.01.005
36. Stenberg, T., et al. (2017), *Quality control and assurance in fabrication of welded structures subjected to fatigue loading*, Weld. World, 61(5): 1003-1015. doi: 10.1007/s40194-017-0490-5
37. Lewandowski, J., Rozumek, D. (2016), *Cracks growth in S355 steel under cyclic bending with fillet welded joint*, Theor. Appl. Fract. Mech. 86(PB): 342-350. doi: 10.1016/j.tafmec.2016.09.003
38. Mikulski, Z., Lassen, T. (2019), *Fatigue crack initiation and subsequent crack growth in fillet welded steel joints*, Int. J Fatigue, 120: 303-318. doi: 10.1016/j.ijfatigue.2018.11.014
39. Krasovskyy, A., Virta, A. (2015), *Fatigue life assessment of welded structures based on fracture mechanics*, Int. J Struct. Integr. 6(1): 2-25. doi: 10.1108/IJSI-04-2014-0012
40. Haghani, R., Al-Emrani, M., Heshmati, M. (2012), *Fatigue-prone details in steel bridges*, Buildings, 2(4): 456-476. doi: 10.3390/buildings2040456
41. Barsoum, Z., Samuelsson, J., Jonsson, B., Björkblad, A. (2012), *Fatigue design of lightweight welded vehicle structures: influence of material and production procedures*, Proc. Inst. Mech. Eng. Part B: J Eng. Manuf. 226(10): 1736-1744. doi: 10.1177/0954405412458046
42. Macdonald, K. (Ed.), Fracture and Fatigue of Welded Joints and Structures, Woodhead Publishing, 2011.
43. Kitagawa, H., Takahashi, S. (1976), *Applicability of fracture mechanics to very small cracks*, In: Proc. 2nd Int. Conf. Mechanical Behavior of Materials, Metals Park, OH: Amer. Soc. Metals, 1976, pp.627-631.
44. Liu, Y., Mahadevan, S. (2009), *Probabilistic fatigue life prediction using an equivalent initial flaw size distribution*, Int. J Fatigue, 31(3): 476-487. doi: 10.1016/j.ijfatigue.2008.06.005
45. Lassen, T. (1990), *The effect of the welding process on the fatigue crack growth*, Weld. J, 69(2): 75S-81S.
46. Dong, Y., Garbatov, Y., Guedes Soares, C. (2018), *A two-phase approach to estimate fatigue crack initiation and propagation lives of notched structural components*, Int. J Fatigue, 116: 523-534. doi: 10.1016/j.ijfatigue.2018.06.049
47. ABS (2003), Guide for Fatigue Assessment of Offshore Structures, updated 2014, Houston, TX, USA, pp.1-56.
48. Zhang, Y.H., Maddox, S.J. (2009), *Fatigue life prediction for toe ground welded joints*, Int. J Fatigue, 31(7): 1124-1136. doi: 10.1016/j.ijfatigue.2009.01.003
49. Krasovskyy, A., Virta, A. (2014), *Fracture mechanics based estimation of fatigue life of welds*, Procedia Eng. 74: 27-32. doi: 10.1016/j.proeng.2014.06.218
50. Maddox, S.J. (1974), *Assessing the significance of flaws in welds subject to fatigue*, Weld. J, 52(9): 401-409.
51. Okawa, T., Shimanuki, H., Nose, T., Suzuki, T. (2013), *Fatigue life prediction of welded structures based on crack growth analysis*, Nippon Steel Tech. Rep. no. 102: 51-53.
52. Hobbacher, A.F. (2009), *The new IIW recommendations for fatigue assessment of welded joints and components - A comprehensive code recently updated*, Int. J Fatigue, 31(1): 50-58. doi: 10.1016/j.ijfatigue.2008.04.002
53. Lautrou, N., Thevenet, D., Cognard, J.Y. (2009), *Fatigue crack initiation life estimation in a steel welded joint by the use of a two-scale damage model*, Fatigue Fract. Eng. Mater. Struct. 32 (5): 403-417. doi: 10.1111/j.1460-2695.2009.01344.x
54. Wen, X., Wang, P., Dong, Z., Fang, H. (2019), *A fracture mechanics-based optimal fatigue design method of undermatched HSLA steel butt-welded joints with imperfections*, Appl. Sci. 9(17): 3609. doi: 10.3390/app9173609
55. Kim, J., et al. (2012), *Improvement of crack inspection possibility using gradient directional magnetization and linearly integrated hall sensors*, J Mech. Sci. Technol. 26(11): 3447-3451. doi: 10.1007/s12206-012-0876-7
56. Lu, Z., Xiang, Y., Liu, Y. (2010), *Crack growth-based fatigue-life prediction using an equivalent initial flaw model. Part II: Multiaxial loading*, Int. J Fatigue, 32(2): 376-381. doi: 10.1016/j.ijfatigue.2009.07.013
57. Blochwitz, C., et al. (Eds.), *Fatigue Cracks : Propagation of Short*, In: The Encyclopedia of Materials: Science and Technology, K.H.J. Buschow et al. (Eds.), Pergamon Press, 2001, pp. 2896-2906.
58. Kim, S., Jeong, D., Sung, H. (2018), *Reviews on factors affecting fatigue behavior of high-Mn steels*, Met. Mater. Int. 24(1): 1-14. doi: 10.1007/s12540-017-7459-1
59. Smith, R.A. (Ed.), Fatigue Crack Growth: 30 Years of Progress: Proceedings of a Conference on Fatigue Crack Growth, Pergamon Press, Cambridge, UK, 1986.
60. Berns, H.D., et al. (Eds.), Fatigue Design Handbook, Vol. AE-10, 2nd Ed., SAE, Warrendale, PA, USA, 1988.
61. Forman, R.G., Kearney, V.E., Engle, R.M. (1967), *Numerical analysis of crack propagation in cyclic-loaded structures*, J Basic Eng. 89(3): 459-463. doi: 10.1115/1.3609637
62. Zhiping, Q., Zesheng, Z., Lei, W. (2017), *Numerical analysis methods of structural fatigue and fracture problems*, In: Contact and Fracture Mechanics, P.H. Darji, V.P. Darji (Eds.), Intech Open. doi: 10.5772/intechopen.72285
63. Fett, T. Dietrich, M., Stress Intensity Factors and Weight Functions, Southampton, UK: Computational Mechanics Publ., 1997. doi: 10.5445/KSP/1000007996
64. Prawoto, Y. (2002), *Linear Elastic Fracture Mechanics (LEFM) analysis of the effect of residual stress on fatigue crack propagation rate*, J Fail. Anal. Prev. 2(5): 75-83. doi: 10.1007/BF02715473
65. Farajian, M. (2013), *Welding residual stress behavior under mechanical loading: Henry Granjon prize competition 2012 winner category C: Design and structural integrity*, Weld. World, 57(2): 157-169. doi: 10.1007/s40194-013-0024-8
66. Beghini, M., Bertini, L., Vitale, E. (1994), *Fatigue crack growth in residual stress fields: experimental results and modelling*, Fatig. Fract. Eng. Mater. Struct. 17(12): 1433-1444. doi: 10.1111/j.1460-2695.1994.tb00786.x
67. Hensel, J., et al. (2018), Welding residual stresses as needed for the prediction of fatigue crack propagation and fatigue strength, Eng. Fract. Mech. 198: 123-141. doi: 10.1016/j.engfracmech.2017.10.024

68. Zerbst, U., Madia, M., Vormwald, M., Beier, H.T. (2018), *Fatigue strength and fracture mechanics - A general perspective*, Eng. Fract. Mech. 198: 2-23. doi: 10.1016/j.engfracmech.2017.04.030
69. Madia, M., Zerbst, U., Beier, H.Th., Schork, B. (2018), *The IBESS model - Elements, realisation and validation*, Eng. Fract. Mech. 198: 171-208. doi: 10.1016/j.engfracmech.2017.08.033
70. Servetti, G., Zhang, X. (2009), *Predicting fatigue crack growth rate in a welded butt joint: The role of effective R ratio in accounting for residual stress effect*, Eng. Fract. Mech. 76 (11): 1589-1602. doi: 10.1016/j.engfracmech.2009.02.015
71. Beier, H.T., et al. (2015), *Simulation of fatigue crack growth in welded joints*, Materwiss. Werksttech. 46(2): 110-122. doi: 10.1002/mawe.201400366
72. Urriolagoitia-Sosa, G., et al. (2012), *Using fracture mechanics for determining residual stress fields in diverse geometries*, Ing. e Investig. 32(3): 19-26.
73. Lei, Y., O'Dowd, N.P., Webster, G.A. (2000), *Fracture mechanics analysis of a crack in a residual stress field*, Int. J Fract. 106(3): 195-216. doi: 10.1023/A:1026574400858
74. Lukic, M., Cremona, C. (2001), *Probabilistic assessment of welded joints versus fatigue and fracture*, J Struct. Eng. 127(2): 211-218. doi: 10.1061/(ASCE)0733-9445(2001)127:2(211)
75. Antunes, F.V., Rodrigues, S.M., Branco, R., Camas, D. (2016), *A numerical analysis of CTOD in constant amplitude fatigue crack growth*, Theor. Appl. Fract. Mech. 85(Part A): 45-55. doi: 10.1016/j.tafmec.2016.08.015
76. Chapetti, M.D., Steimbreger, C. (2019), *A simple fracture mechanics estimation of the fatigue endurance of welded joints*, Int. J Fatigue, 125: 23-34. doi: 10.1016/j.ijfatigue.2019.03.021
77. He, C., Liu, Y., Fang, D., Wang, Q. (2012), *Very high cycle fatigue behavior of bridge steel welded joint*, Theor. Appl. Mech. Lett. 2(3): 031010. doi: 10.1063/2.1203110
78. Masubuchi, K., Analysis of Welded Structures: Residual Stresses, Distortion, and Their Consequences, D.W. Hopkins (Ed.), Pergamon Press, 1980.
79. Dowling, N.E., Mechanical Behavior of Materials: Engineering Methods for Deformation, Fracture, and Fatigue, 4th Ed., Pearson Education Ltd., England, 2013.
80. Pollak, R.D., Analysis of methods for determining high cycle fatigue strength of a material with investigation of Ti-6Al-4V gigacycle fatigue behavior, Doctoral Thesis, Air Force Inst. of Technol., 2005, p. 278.
81. Paris, P.C, Gomez, M.P., Anderson, W.E. (1961), *A rational analytic theory of fatigue*, The Trend in Eng. 13: 9-14.
82. Wang, W., Cheng-Tzu, T.H. (1994), *Fatigue crack growth rate of metal by plastic energy damage accumulation theory*, J Eng. Mech. 120(4): 776-795.
83. Beden, S.M., Abdullah, S., Ariffin, A.K. (2009), *Review of fatigue crack propagation models for metallic components*, Eur. J Sci. Res. 28(3): 364-397.
84. Zhu, X.K., Joyce, J.A. (2012), *Review of fracture toughness (G, K, J, CTOD, CTOA) testing and standardization*, Eng. Fract. Mech. 85: 1-46. doi :10.1016/j.engfracmech.2012.02.001
85. Carpinteri, A., Ronchei, C., Scorza, D., Vantadori, S. (2015), *Fracture mechanics based approach to fatigue analysis of welded joints*, Eng. Fail. Anal. 49(C): 67-78. doi: 10.1016/j.engfailanal.2014.12.021
86. Mikkola, E., Murakami, Y., Marquis, G. (2014), *Fatigue life assessment of welded joints by the equivalent crack length method*, Procedia Mater. Sci. 3: 1822-1827. doi: 10.1016/j.mspro.2014.06.294
87. Shen, W., Choo, Y.S. (2012), *Stress intensity factor for a tubular T-joint with grouted chord*, Eng. Struct. 35: 37-47. doi: 10.1016/j.engstruct.2011.10.014
88. Nguyen, N.T., Wahab, M.A. (1996), *The effect of undercut, misalignment and residual stresses on the fatigue behaviour of butt welded joints*, Fatigue Fract. Eng. Mater. Struct. 19(6): 769-778. doi: 10.1111/j.1460-2695.1996.tb01321.x
89. Mecséri, B.J., Kövesdi, B. (2017), *Crack propagation modelling for high strength steel welded structural details*, J Phys. Conf. Ser. 843(1): 012045. doi: 10.1088/1742-6596/843/1/012045
90. Chauhan, S., Pawar, A.K., Chattopadhyay, J., Dutta, B.K. (2016), *Determination of fatigue properties using miniaturized specimens*, Trans. Indian Inst. Met. 69(2): 609-615. doi: 10.1007/s12666-015-0796-1
91. Luke, M., Varfolomeev, I., Lütkepohl, K., Esderts, A. (2011), *Fatigue crack growth in railway axles: Assessment concept and validation tests*, Eng. Fract. Mech. 78(5): 714-730. doi: 10.1016/j.engfracmech.2010.11.024
92. Milović, L., et al. (2011), *Determination of fatigue crack growth parameters in welded joint of HSLA steel*, Struct. Integr. and Life, 11(3): 183-187.
93. Deliou, A., Bouchouicha, B. (2018), *Fatigue crack propagation in welded joints X70*, Frat. ed Integrita Strutt. 12(46): 306-318. doi: 10.3221/IGF-ESIS.46.28
94. Maier, B., Guster, Ch., Tichy, R., Ecker, W. (2013), *Influence of different microstructures of the welding zone on the fatigue crack growth behaviour of HSLA steels*, 13th Int. Conf. Fract. ICF 2013, Beijing, China, 2013, vol.5, pp. 4170-4176.
95. Vargas-Arista, B., et al. (2013), *Normalizing effect on fatigue crack propagation at the heat-affected zone of AISI 4140 steel shielded metal arc weldings*, Mater. Res. 16(4): 772-778. doi: 10.1590/S1516-14392013005000047
96. Chapetti, M.D., Otegui, J.L. (1997), *A technique to produce automatic welds with enhanced fatigue crack propagation lives under transverse loading*, Int. J Press. Ves. Piping 70(3): 173-181. doi: 10.1016/S0308-0161(96)00028-2
97. Alam, M.S., Structural integrity and fatigue crack propagation life assessment of welded and weld-repaired structures, Doctoral Thesis, Louisiana State University, 2005.
98. Billingham, J., Sharp, J.V., Spurrier, J., Kilgallon, P.J., *Review of the performance of high strength steels used offshore*, RR 105, Cranfield Univers. Health Safety Executive, 2003, p.130.
99. Marquis, G. (2010), *Failure modes and fatigue strength of improved HSS welds*, Eng. Fract. Mech. 77(11): 2051-2062. doi: 10.1016/j.engfracmech.2010.03.034
100. Nordin, N., et al. (2019), *Residual stress assessment of PWMT butt joint with 10mm HSLA S460G2+M steel using HFMI/PIT FEA and XRD*, MATECT Web Conf. 269: 03010. doi: 10.1051/matecconf/201926903010
101. Saidin, S., et al. (2019), *Effects of high frequency mechanical impact on fatigue life of semi-automated gas metal arc welding (GTAW) of HSLA butt*, MATEC Web Conf. 269: 06002. doi: 10.1051/matecconf/201926906002
102. Andud, D., et al. (2019), *Fatigue life enhancement of transverse and longitudinal T-joint on offshore steel structure HSLA S460G2+M using semi-automated GMAW and HFMI/PIT*, MATEC Web Conf. 269(3): 06001. doi: 10.1051/matecconf/201926906001
103. Čabrilo, A., Sedmak, A., Burzić, Z., Perković, S. (2019), *Fracture mechanics and fatigue crack propagation in armor steel welds*, Eng. Fail. Anal. 106: 104155. doi: 10.1016/j.engfailanal.2019.104155
104. Čabrilo, A., Cvetinov, M. (2017), *Fatigue crack propagation and Charpy impact properties in armor steel welds*, Mater. Plast. 54(4): 601-806. doi: 10.37358/MP.17.4.4927
105. Ravi, S., Balasubramanian, V., Nemat Nasser, S. (2004), *Effect of mis-match ratio (MMR) on fatigue crack growth behaviour of HSLA steel welds*, Eng. Fail. Anal. 11(3): 413-428. doi: 10.1016/j.engfailanal.2003.05.013

106. Payares-Asprino, M.C., Katsumoto, H., Liu, S. (2008), *Effect of martensite start and finish temperature on residual stress development in structural steel welds*, Weld. J, 87(11): 279s-289s.
107. Harati, E., Karlsson, L., Svensson, L.E., Dalaei, K. (2017), *Applicability of low transformation temperature welding consumables to increase fatigue strength of welded high strength steels*, Int. J Fatigue, 97(C): 39-47. doi: 10.1016/j.ijfatigue.2016.12.007
108. Ramjaun, T.I., et al. (2014), *Surface residual stresses in multi-pass welds produced using low transformation temperature filler alloys*, Sci. Technol. Weld. Join. 19(7): 623-630. doi: 10.1179/1362171814Y.0000000234
109. Karlsson, L., Mráz, L., Bhadeshia, H.K.D.H., Shirzadi, A. (2010), *Comparison of alloying concepts for Low Transformation Temperature (LTT) welding consumables*, Biul. Inst. Spaw. 5(5): 33-39.
110. Zenitani, S., et al. (2007), *Development of new low transformation temperature welding consumable to prevent cold cracking in high strength steel welds*, Sci. Technol. Weld. Join. 12(6): 516-522. doi: 10.1179/174329307X213675
111. Ohta, A., et al. (1999), *Superior fatigue crack growth properties in newly developed weld metal*, Int. J Fatigue, 21: S113-S118.
112. Lukács, J., Dobosy, Á. (2019), *Matching effect on fatigue crack growth behaviour of high-strength steels GMA welded joints*, Weld. World, 63(5): 1315-1327. doi: 10.1007/s40194-019-00768-3
113. Ottersböck, M.J., Leitner, M., Stoschka, M., Maurer, W. (2019), *Crack initiation and propagation fatigue life of ultra high-strength steel butt joints*, Appl. Sci. 9(21): 4590. doi: 10.3390/app9214590
114. Ermi, A.M., James, L.A. (1986), *Miniature center-cracked-tension specimen for fatigue crack growth testing*, In: The use of small-scale specimens for testing irradiated material, ASTM STP 888. Philadelphia, PA, USA, 1986, pp.261-275.
115. Karthik, V., Kasiviswanathan, K.V., Raj, B. (2016), *Miniature specimens for fatigue and fracture properties*, In: Miniaturized Testing of Engineering Materials, CRC Press, 2016: 84-109.
116. Li, M., Stubbins, J. (2002), *Subsize specimens for fatigue crack growth rate testing of metallic materials*, In: Small Specimen Test Techniques, Vol.4, M. Sokolov, J. Landes, G. Lucas (Eds.) ASTM Int., West Conshohocken, PA, 2002, pp.321-335. doi: 10.1520/STP10830S
117. Beretta, S., Carboni, M. (2011), *Variable amplitude fatigue crack growth in a mild steel for railway axles: Experiments and predictive models*, Eng. Fract. Mech. 78(5): 848-862. doi: 10.1016/j.engfracmech.2010.11.019
118. ISO 27306:2016, Metallic materials - Method of constraint loss correction of CTOD fracture toughness for fracture assessment of steel components.
119. Berdnikova, O., et al. (2019), *Effect of the structure on the mechanical properties and cracking resistance of welded joints of low-alloyed high-strength steels*, Procedia Struct. Integ. 16: 89-96. doi: 10.1016/j.prostr.2019.07.026
120. Bayley, C. (2015), *Evaluation of the single edge notch tension specimen for quantifying fracture toughness*, Partic. in a round-robin test program, Sci. Rep. DRDC-RDDC-2015-R156, 2015.
121. Verstraete, M.A., De Waele, W., Van Minnebruggen, K., Hertelé, S. (2015), *Single-specimen evaluation of tearing resistance in SENT testing*, Eng. Fract. Mech. 148: 324-336. doi: 10.1016/j.engfracmech.2015.07.067
122. Ruggieri, C. (2012), *Further results in J and CTOD estimation procedures for SE(T) fracture specimens - Part I: Homogeneous materials*, Eng. Fract. Mech. 79: 245-265. doi: 10.1016/j.engfracmech.2011.11.003
123. Marcelo, L., Tobar, P., Ruggieri, C. (2009), *Estimation procedure of J and CTOD fracture parameters for SE(T) fracture specimens based on the η method*, In: Proc. COBEM, 20th Int. Cong. Mech. Eng. Gramado, Brazil, 2009.
124. Fredriksson, E., Accuracy Study in Predicting Fatigue Life for a Welding Joint, KTH Eng. Sci., Stockholm, Sweden, 2015.
125. Friedrich, N., Ehlers, S. (2019), *A simplified welding simulation approach used to design a fatigue test specimen containing residual stresses*, Ship Technol. Res. 66(1): 22-37. doi: 10.1080/09377255.2018.1518692
126. Kazemzadeh-Parsi, M.J., Daneshmand, F. (2010), *Cavity-shape identification with convective boundary conditions using non-boundary-fitted meshes*, Numer. Heat Transf. Part B: Fundam. 57(4): 283-305. doi: 10.1080/10407790.2010.481496
127. Al-Mukhtar, A., Biermann, H., Henkel, S., Hubner, P. (2009), *A finite element calculation of stress intensity factors of cruciform and butt welded joints for some geometrical parameters*, Jordan J. Mech. Ind. Eng. 3(4): 236-245.
128. Reddy, J.N., An Introduction to Nonlinear Finite Element Analysis, 2nd Ed., with applications to heat transfer, fluid mechanics, and solid mechanics, Oxford Univ. Press, 2014. doi: 10.1093/acprof:oso/9780199641758.001.0001
129. Fazeli, H., Mirzaei, M. (2012), *Shape identification problems on detecting of defects in a solid body using inverse heat conduction approach*, J Mech. Sci. Technol. 26(11): 3681-3690. doi: 10.1007/s12206-012-0842-4
130. Schijve, J., Fatigue of Structures and Materials, Kluwer Academic Publishing, 2009. doi: 10.1007/978-1-4020-6808-9
131. Yang, Y., Vormwald, M. (2017), *Fatigue crack growth simulation under cyclic non-proportional mixed mode loading*, Int. J Fatigue, 102(C): 37-47. doi: 10.1016/j.ijfatigue.2017.04.014
132. Zerbst, U., et al. (2014), *Review on fracture and crack propagation in weldments - A fracture mechanics perspective*, Eng. Fract. Mech. 132: 200-276. doi: 10.1016/j.engfracmech.2014.05.012
133. Baik, B., Yamada, K., Ishikawa, T. (2011), *Fatigue crack propagation analysis for welded joint subjected to bending*, Int. J Fatigue, 33(5): 746-758. doi: 10.1016/j.ijfatigue.2010.12.002
134. Ghafoori Ahangar, R., Verreman, Y. (2019), *Assessment of mode I and mode II stress intensity factors obtained by displacement extrapolation and interaction integral methods*, J Fail. Anal. Prev. 19(1): 85-97. doi: 10.1007/s11668-018-0571-9
135. Guo, L., Xiang, J., Latham, J.P., Izzuddin, B. (2016), *A numerical investigation of mesh sensitivity for a new three-dimensional fracture model within the combined finite-discrete element method*, Eng. Fract. Mech. 151: 70-91. doi: 10.1016/j.engfracmech.2015.11.006
136. Al-Mukhtar, A., Biermann, H., Hübner, P., Henkel, S. (2009), *Fatigue crack propagation life calculation in welded joints*, In: CP2009: 391-397.
137. Dong, Y., Guedes Soares, C. (2019), *Stress distribution and fatigue crack propagation analyses in welded joints*, Fatigue Fract. Eng. Mater. Struct. 42(1): 69-83. doi: 10.1111/ffe.12871
138. Araque, O., Arzola, N., Varón, O. (2019), *Computational modeling of fatigue crack propagation in butt welded joints subjected to axial load*, PLoS One, 14(6): 1-17. doi: 10.1371/journal.pone.0218973
139. Stenberg, T., Barsoum, Z., Hedlund, J., Josefsson, J. (2019), *Development of a computational fatigue model for evaluation of weld quality*, Weld. World, 63(6): 1771-1785. doi: 10.1007/s40194-019-00777-2